chemosensors

MDPI

Review

Smart Contact Lens Sensors for Ocular Health Monitoring: Advances in Materials, Fabrication and Application

Lichun Gao [1,†], Jiancheng Dong [2,†] and Yang Wang [2,*]

[1] School of Management, Wuhan University of Technology, Wuhan 430070, China; ylgaolichun@126.com
[2] Key Laboratory of Biomechanics and Mechanobiology, Ministry of Education, Beijing Advanced Innovation Center for Biomedical Engineering, School of Engineering Medicine, Beihang University, Beijing 100191, China; dongjiancheng11@163.com
* Correspondence: wangyang2022@buaa.edu.cn; Tel.: +86-156-0061-5669
† These authors contributed equally to this work.

Abstract

Smart contact lens sensors integrate biochemical sensing elements, flexible electronics, power modules, and wireless readout components onto optically transparent contact lens platforms, enabling non-invasive and potentially continuous analysis of tear-derived biomarkers and ocular physiological signals. This review focuses on the translation pathway from contact lens materials and fabrication methods to sensing mechanisms, tear biomarker interpretation, and clinical deployment. We synthesize recent progress in substrate engineering, manufacturing processes, power delivery, and representative sensing strategies for intraocular pressure, glucose, electrolytes, pH, cortisol, cholesterol, and inflammatory cytokines. Instead of treating these systems as isolated examples, we compare optical/colorimetric, electrochemical, field-effect transistor, microfluidic, and wireless resonant approaches in terms of sensitivity, response time, power/readout requirements, and clinical relevance. Finally, we discuss persistent barriers, including biocompatibility, interface stability, tear-sample variability, calibration, sterilization, regulatory validation, data privacy, and compatibility with commercial contact lens manufacturing.

Keywords: smart contact lenses; sensor; tear analysis; biomarker

1. Introduction

With socioeconomic development and accelerating population aging, the demand for health monitoring has shown a marked growth trend. Wearable bioelectronic devices, which can be used for out-of-hospital- and self-monitoring, represent an important direction in the development of medical diagnostic and therapeutic devices. Innovative research targeting chronic disease management (blood glucose monitoring, electrocardiography) and vital sign monitoring (heart rate, blood pressure, blood oxygen saturation) has emerged continuously, with the aim of achieving non-invasive, continuous, and real-time detection of human physiological signals and disease biomarkers without interfering with the wearer's daily activities [1–3]. Wearable bioelectronic devices integrate signal acquisition and data analysis into a single platform, delivering timely and accurate results, and serving as a precision paradigm for realizing "one person–one strategy" personalized health management [4,5].

Traditional detection and diagnosis of ophthalmic diseases mainly rely on discrete clinical examinations, such as tonometry, corneal topography, or tear biochemical analysis. These methods not only require specialized equipment and trained personnel but also

Check for updates

Received: 13 May 2026
Revised: 8 June 2026
Accepted: 14 June 2026
Published: 17 June 2026

Copyright: © 2026 by the authors. Licensee MDPI, Basel, Switzerland. This article is an open access article distributed under the terms and conditions of the Creative Commons Attribution (CC BY) license.

struggle to achieve long-term, continuous physiological data acquisition. However, the pathological changes in many ocular diseases (such as glaucoma and dry eye syndrome) and systemic diseases (such as diabetes) exhibit dynamic fluctuation characteristics. Relying solely on single or intermittent measurements may miss critical information, thereby compromising early diagnosis and precise treatment. The rise in smart contact lenses provides an innovative solution to this problem. By integrating miniaturized biochemical sensors, wireless communication modules, and flexible circuits onto a contact lens substrate, smart contact lenses can monitor physical parameters such as intraocular pressure [6–9], ocular surface temperature [10], and pH [11] in real time, and analyze biochemical markers such as glucose [12,13], cortisol [14], and cytokines [15] in tear fluid—all without impairing normal visual function. This non-invasive, continuous monitoring approach not only improves the temporal resolution of data but also lays the foundation for personalized medicine and remote health management [16,17].

This paper systematically reviews the technical principles, current application status, and future trends of smart contact lens sensors for ocular and tear biomarker detection (Figure 1). Centered on biomarker monitoring, the review presents in turn the evolution of contact lens materials and fabrication processes as enabling foundations, the sensing mechanisms that convert biomarker-related information into readable optical or electrical signals, the latest advances in different biomarker-detection applications, and the current technical bottlenecks and commercialization challenges that limit clinical translation, with the aim of providing a structured reference for subsequent research.

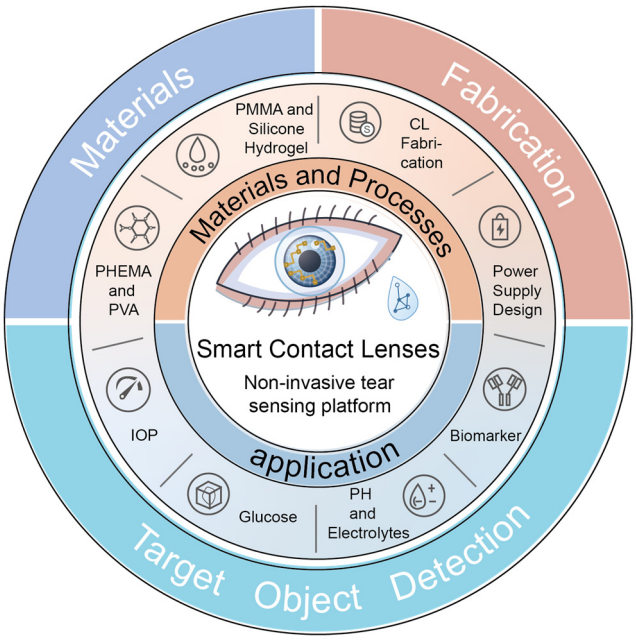


Figure 1. Smart contact lenses.

2. Materials and Fabrication Processes

As for the platform and substrate of smart contact lenses, scientists have made numerous attempts and innovations in the material selection and design of contact lenses to improve their physical properties—including optical transparency, structural strength, stability, and oxygen permeability—in order to reduce discomfort during wear. When used to host sensors and integrated circuits to form novel smart contact lenses, additional considerations such as material wettability, electronic device compatibility, and biocompatibility must be taken into account. This section systematically outlines the evolutionary path

of substrate materials and manufacturing processes under multiple performance requirements, and introduces the primary power delivery designs applied in smart contact lenses.

2.1. Materials and Manufacturing

Although early PMMA possessed excellent optical transparency, elastic modulus, and durability [18,19], its extremely low oxygen permeability led to corneal hypoxia, which could further trigger ocular health issues such as corneal neovascularization [20]. This drawback in wearing comfort caused it to gradually fade from the mainstream market [21]. Due to their inherent robust siloxane bonding structure, silicone hydrogels possess natural oxygen permeability and durability [20]. These characteristics make contact lenses made from silicone hydrogels highly durable and commercially viable, accounting for approximately 81% of the global soft contact lens market in 2024 [22]. However, the intrinsic hydrophobicity of the silicone material results in poor surface wettability of the lenses, easily causing ocular dryness and discomfort, and its higher modulus compared to conventional hydrogels can also irritate the eye [23,24]. To address this core conflict between high oxygen permeability and hydrophobicity, researchers have carried out extensive surface modification work [25]. Wang et al. [26] grafted 2-methacryloyloxyethyl phosphorylcholine (MPC) onto silicone hydrogels via UV-induced free radical polymerization, obtaining a hydrophilic surface with a water contact angle as low as 20° without compromising oxygen permeability or tensile strength. The following year, the same team used UV induction to graft poly(ethylene glycol) methyl ether acrylate (PEGMA) onto the silicone hydrogel surface, improving hydrophilicity without reducing transparency, oxygen permeability, or modulus [27]. Ivan Melendez-Ortiz et al. [25] reported a method of grafting PVCL and PMAA onto silicone-based films using γ-ray pre-irradiation, demonstrating low affinity for bovine serum albumin and fibrinogen and excellent anti-fouling effects. At the commercialization level, plasma treatment [28] is a common approach to improve contact lens wettability. Paul L et al. [29] proposed a method that generates an optically transparent hydrophilic coating on the contact lens surface by plasma oxidation followed by the attachment of hydrophilic polymer chains.

As shown in Figure 2a,b, PHEMA [30] and PVA [31–33] provide two alternative choices for smart contact lens substrates. PHEMA hydrogels have a relatively high water content (HEMA-only hydrogels contain approximately 38% water [20]), offering a comfortable wearing experience, and their derivative hydrogels constitute an important part of the market [34,35]. Studies have shown that copolymerizing HEMA with monomers such as NVP, MA, and GMA can improve the surface wettability and structural stability of the polymer, but crosslinking molecules such as ethylene glycol dimethacrylate (EGDMA) need to be introduced to enhance mechanical properties, which sacrifices oxygen transmissibility to some extent [36–38]. Moreover, PHEMA-based hydrogels face problems of protein deposition and bacterial adhesion [39], and antimicrobial strategies as well as wettability retention techniques still require further development [40,41]. PVA is a relatively newer polymer, with a single hydroxyl group present in each repeating monomer unit, endowing it with excellent hydrophilicity and biocompatibility [42,43]. Even without modification, it exhibits lower protein absorption and higher tensile strength compared to other materials [44]. However, low oxygen permeability limits the application of PVA, and improving this shortcoming through surface modification remains a necessary research direction.

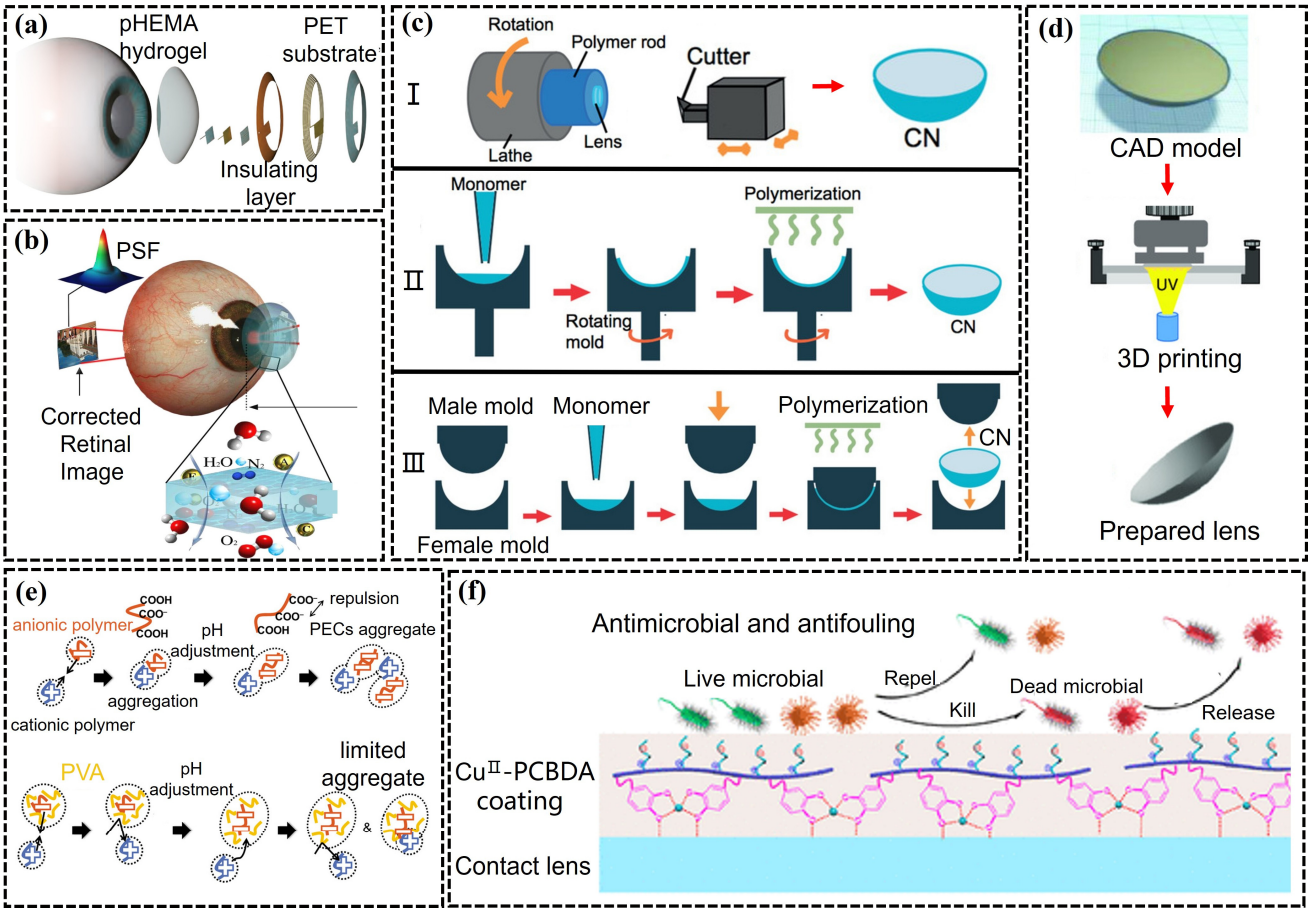


Figure 2. (**a**) Smart contact lenses based on PHEMA [30]. The smart contact lens is composed of a pHEMA hydrogel substrate and functional devices (an inductance coil and a pyramid-microstructured parallel-plate capacitive pressure sensor). (**b**) Smart contact lenses based on PVA [31]. (**c**) Manufacturing process of smart contact lenses, (**I**) lathe-cut method [45], (**II**) spin-casting method [45], (**III**) injection-molding method [45], (**d**) 3D printing [46]. (**e**) Self-assembly multilayer polyelectrolyte solves the hydrophobicity of silicone hydrogels [47]. (**f**) The zwitterionic Cu^{II}–PCBDA coating exhibits both antimicrobial and antifouling properties [48].

When further integrating electronic components, the modulus mismatch between rigid sensors and chips and the soft corneal curvature becomes a new prominent conflict. To mitigate this problem, researchers have sought breakthroughs at both the material mechanics and manufacturing process levels. At the material level, stretchable transparent electrodes—such as the continuous random network of ultra-long silver nanofibers (AgNF) fabricated by electrospinning on PDMS by Jang et al. [49], and the kirigami structure [9] design reported by Chen et al.—can achieve high stretchability and corneal compliance without sacrificing conductive performance. At the manufacturing process level, 3D printing, as a typical additive manufacturing technology, has become an emerging approach for fabricating smart contact lenses [46,50,51]. It offers the advantages of a short fabrication time and low cost, and can precisely control dimensions without shape limitations [17]. Particularly in the fabrication of smart contact lenses, it enables the construction of structures at the microscale, realizing the embedding of microsensors, controllers, and integrated circuits. As shown in Figure 2c,d, Ghada Zidan et al. [52] conducted a comparative study of casting and 3D printing methods for preparing gelatin hydrogel drug-eluting contact lenses, and the results showed that 3D printing technology increased the swelling ratio, thereby leading to rapid drug release. In contrast, the three traditional manufacturing techniques—lathe cutting, spin casting, and injection molding—although still applied in

conventional contact lens production, have inherent limitations when handling heterogeneous material integration [45]. The lathe cutting method can readily counteract surface degradation during cutting and achieve automated processing [53,54], but is relatively time-consuming [21]; the spin casting method can quickly produce relatively thin finished products, but requires anaerobic conditions and nitrogen purging to reduce irreversible surface degradation effects [45,54]; injection molding, currently the most commonly used method, hardens the material by pressing two molds together, offering low cost and avoiding the polishing process [55].

The third core conflict faced during long-term wear is biocompatibility—protein deposition and bacterial adhesion not only reduce optical transparency, but may also trigger infection and lead to sensor performance degradation. To address this issue, as shown in Figure 2e,f, multilayer polyelectrolyte self-assembled layers [47] and zwitterionic coatings [48,56] effectively suppress nonspecific protein adsorption and bacterial growth. The design of antibacterial hydrogels (e.g., doped with silver nanoparticles) further enhances wearing safety. These surface engineering strategies serve as crucial support for transitioning smart contact lenses from the laboratory to clinical application, and from short-term testing to long-term wear.

2.2. Power Delivery Design

Beyond their vision-correcting function, smart contact lenses further provide capabilities such as sensing and drug delivery. To ensure the proper realization of these intended functions, the power delivery method must not interfere with the wearer's normal activities, thus necessitating careful design of the power module [57]. One standard approach is to use flexible conductive wires to connect the built-in components of the smart contact lenses to an external power source [58–61]. For example, Fan et al. [60] designed a smart contact lenses for intraocular pressure monitoring based on a piezoresistive pressure sensor, in which a semiconductor parameter analyzer in the experimental setup supplied a constant current to the sensor via wires. This method is only suitable for the laboratory development stage of smart contact lenses and can cause significant inconvenience and discomfort to the wearer. In addition to using wired methods for power supply, as shown in Figure 3a, Lee's team [62] provided an aqueous battery strategy based on tear fluid and Prussian blue nanocomposites, which can deliver a discharge capacity of 155 μAh in tear fluid containing 0.15 M sodium ions and 0.02 M potassium ions, sufficient to power a low-power microprocessor. Therefore, wireless power delivery strategies are more appropriate for the future development of smart contact lenses [63,64]. As shown in Figure 3b, Park et al. [12] designed an NFC-based wireless smart contact lens for continuous monitoring of glucose levels in tear fluid at sub-minute resolution. This study fabricated a resonant coil on the contact lens substrate using MEMS technology, enabling wireless power delivery to the built-in sensor and allowing data transmission with sufficient bandwidth. Although this method of wireless power delivery and data transmission using radio frequency signals avoids the non-compliance issues associated with wires, the antenna design still faces limitations in terms of size and the unavoidable effect of Joule heating. Furthermore, as shown in Figure 3c, ultrasonic power transmission [65–67] represents another potential approach to realize wireless and passive functionality in smart contact lenses, relying on an ultrasonic oscillator in the 200 kHz to 1.2 MHz frequency range and an ultra-miniature piezoelectric transducer embedded inside the smart contact lens. The deep penetration and low bioabsorption characteristics of ultrasound give it unique advantages in implantable medical devices, though its application in the smart contact lens field is still at the exploratory stage.

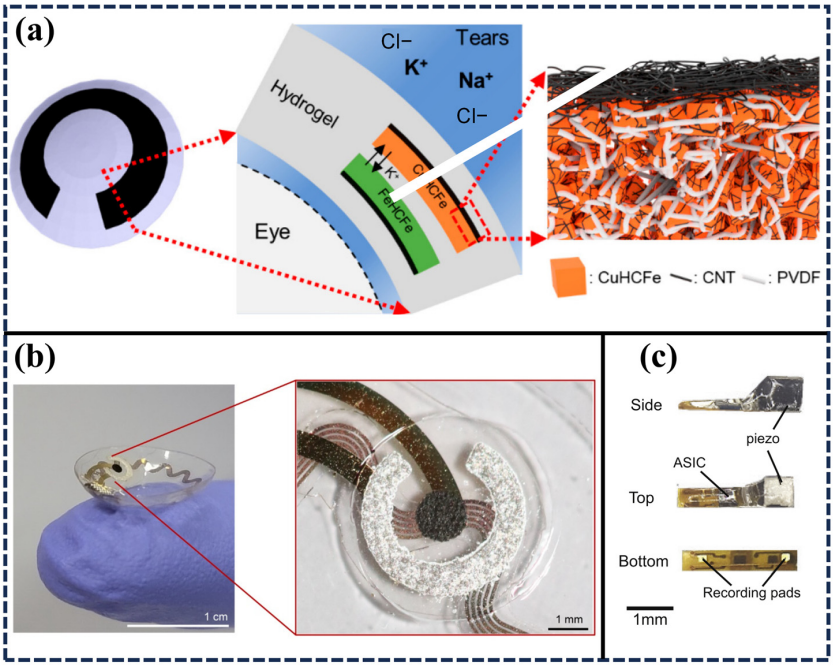


Figure 3. Energy supply design for smart contact lenses. (**a**) Schematic of the battery made of porous electrodes and hydrogel [62]. Porous electrodes consisted of PBA nanoparticles, CNT, and PVDF are placed in the hydrogel. (**b**) Photograph of an integrated smart contact lens with an exposed glucose sensor and NFC module (**left**), and optical micrograph of the exposed glucose sensor (**right**) [12]. (**c**) Ultrasound-generating components assembled on a flexible printed circuit board, comprising a piezoelectric crystal, a custom single transistor and a pair of recording electrodes [65].

3. Applications

Wearable devices that utilize body fluids such as sweat [68–70], tears [71,72], saliva [73], and urine [74,75] for health monitoring have attracted increasing attention due to their non-invasive, continuous, and real-time capabilities [76,77]. Among these biofluids, tears are particularly suitable for smart contact lens sensors because they are naturally present at the ocular surface, can be accessed directly by a contact lens without additional sampling, and contain metabolites, electrolytes, proteins and inflammatory mediators associated with systemic and ocular conditions. The optical transparency and conformal contact of soft lenses further enable continuous monitoring of tear biomarkers and ocular physiological parameters, such as intraocular pressure, with minimal interference to vision or daily wear. Therefore, smart contact lens sensors provide a dedicated platform for tear-based and ocular health monitoring. This section summarizes recent advances in smart contact lens sensors for disease diagnostics based on tear biomarkers and ocular parameters [57].

3.1. IOP

Intraocular pressure (IOP) refers to the fluid pressure within the eye, determined by measuring the force exerted by the aqueous humor on the anterior inner surface of the eye. It is regulated through a balance between the production and drainage of aqueous humor to maintain the structural integrity of the globe [78]. Glaucoma is a progressive optic neuropathy caused by impaired drainage at the trabecular meshwork, leading to vision loss and other complications, with elevated IOP being a major pathological feature [79,80]. Therefore, IOP is an important clinical parameter for the diagnosis and treatment of glaucoma. Since Detry-Morel, M [81] first mentioned smart contact lens sensors as a means of measuring IOP on the corneal surface in 2007, research reports in this application field have been steadily growing [82,83].

To avoid the mechanical mismatch, reduced oxygen permeability, and long-term wearing discomfort associated with traditional electronic components in contact lenses, visualization-based IOP sensing strategies that eliminate electronic elements have gradually attracted attention [84–87]. As shown in Figure 4a, Moreddu et al. [88] developed an optomechanical IOP sensor that uses a stretchable PDMS nanopillar array as a strain-tunable diffraction grating and integrates it into a soft contact lens. When IOP changes induce minute deformations of the cornea and the lens, the grating pitch varies with strain, thereby altering the diffraction pattern and reflected color, enabling optical readout of IOP-related strain. The sensor exhibited a linear response in the range of 15–35 mmHg with a detection limit below 2 mmHg, and a portable readout method based on smartphone color recognition was proposed, offering a new technical pathway for electronics-free IOP monitoring. However, optical color readout is susceptible to factors such as ambient light, imaging angle, and iris color, limiting its quantitative stability in the complex ocular surface environment. Unlike approaches that rely on changes in optical nanostructures, microfluidic sensors achieve visual amplification of IOP signals through liquid interface displacement. As shown in Figure 4b, Sevda et al. [84] designed a passive integrated microfluidic sensor that transduces subtle IOP-induced stress variations into fluid expansion and contraction, enabling quantitative readout with a smartphone camera. Using this design, the authors implanted the smart contact lens sensor in a porcine eye and continuously monitored IOP-induced strain for at least 19 h. Leveraging the advantages of microfluidic sensors in flexibility, low cost, and visual readout, Yu et al. [86] designed a microfluidic smart contact lens sensor based on a bilateral-wall structure. The unique bilateral-wall design significantly enhanced the sensitivity and linearity of the sensor, and with the integrated automated image processing program, automatic acquisition of the liquid interface displacement and visual readout of IOP were achieved. Although this sensor offers high sensitivity, it relies on external image processing and a high-resolution camera. To address these issues, Kouhani et al. [89] developed a closed-loop serpentine wireless passive sensor that tracks IOP-induced corneal curvature changes through resonant-frequency shifts, advancing non-invasive continuous IOP monitoring towards clinical translation.

MEMS technologies offer high precision and miniaturization, enabling researchers to integrate semiconductor pressure sensors into smart contact lens platforms for detecting IOP fluctuations. The authors developed a non-invasive smart contact lens sensor based on a fiber Bragg grating. They integrated an etched fiber Bragg grating onto a PDMS substrate to detect IOP-induced corneal deformation, achieving a sensitivity of 49.243 pm/mmHg over an IOP range of 0–50 mmHg [90]. Piezoresistive strain sensors utilize the piezoresistive effect to convert IOP-induced minute deformations of the cornea/contact lens into resistance changes, thereby enabling quantitative monitoring of IOP fluctuations. Hence, integrating them into smart contact lens sensors for IOP monitoring is a feasible approach. As shown in Figure 4c, Shao et al. [10] proposed a tonometer based on Si-NR, capable of accurately detecting IOP fluctuations in ex vivo porcine eyes and in vivo rabbit eyes, with an integrated ocular temperature sensor for temperature compensation, which is beneficial for glaucoma diagnosis. However, this study did not eliminate the constraint of external wires, limiting its application in daily long-term monitoring. To realize a wireless and wearable IOP-monitoring system, Kim et al. [91] developed a soft, transparent smart contact lens that integrates monocrystalline silicon nanomembrane piezoresistive strain sensors with an NFC chip, a transparent stretchable antenna, capacitors, resistors and three-dimensional liquid-metal interconnects. By concentrating minute IOP-induced corneal deformations onto the silicon strain-sensor region through a rigid–soft hybrid structure, the device enabled wireless, battery-free smartphone readout via NFC and demonstrated the feasibility of integrating silicon-based piezoresistive sensors into wearable continuous

IOP-monitoring systems. Although this strategy improved wireless readout capability, the device structure and on-chip interconnects remained relatively complex. Therefore, to further reduce the need for active on-chip components and complex interconnects, Li et al. [92] proposed a wireless passive smart contact lens based on a dual inductor–capacitor–resistor (LCR) resonant circuit as shown in Figure 4d. IOP fluctuations altered the corneal and contact-lens curvature, changed the inductance of the spiral coil and shifted the resonant frequency, which an external readout coil detected wirelessly. The device enabled highly linear IOP detection over 10–50 mmHg in ex vivo porcine eyes, with sensitivities of 0.112 and 0.186 MHz $mmHg^{-1}$ for the low-frequency and high-frequency resonators, respectively. It maintained an average relative error of ~6.62% under temperature fluctuations exceeding 10 °C, highlighting its potential for next-generation all-day IOP monitoring.

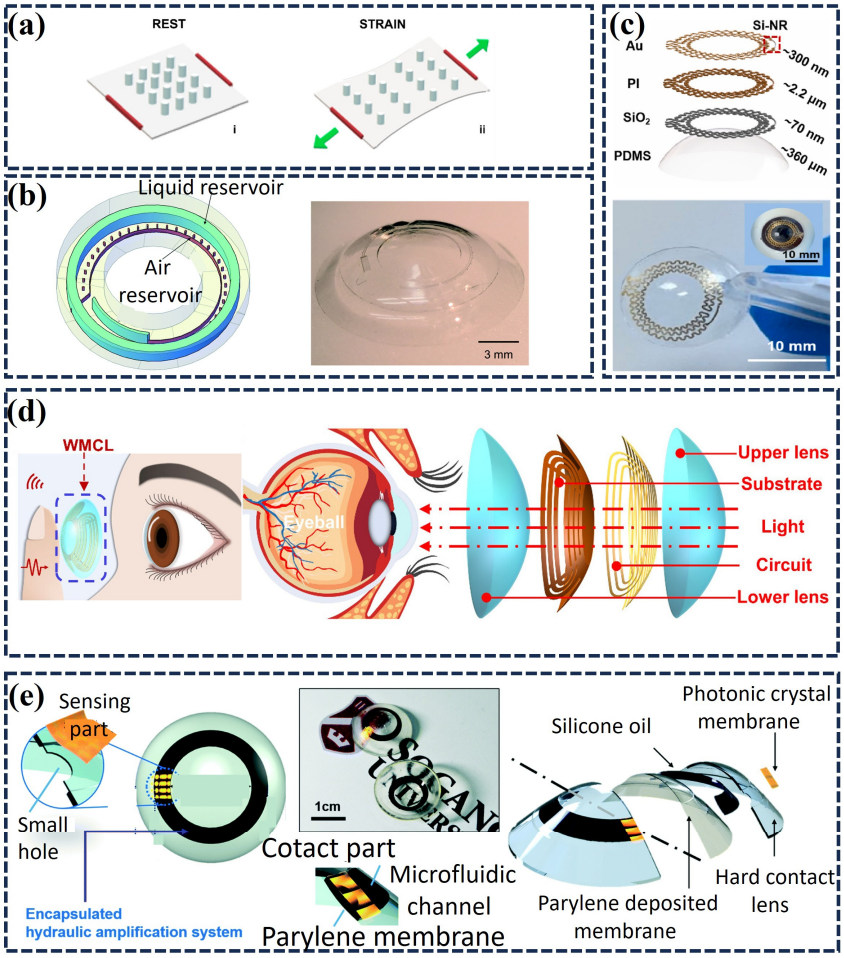


Figure 4. Application of smart contact lenses in IOP detection. (**a**) The working principle of strain sensors. (**i**) Left image: The sensor is in a stationary state. (**ii**) Right picture: The sensor is in a stressed state [88]. (**b**) 3D schematic diagram and physical image of strain sensor [84]. The sensor is composed of a liquid reservoir and an air reservoir. (**c**) Structure diagram and physical image of intraocular pressure meter based on Si-NR [10]. (**d**) Schematic diagram and device structure diagram of wireless intraocular pressure monitoring system WMCL [92]. (**e**) Smart contact lens IOP sensor based on photonic crystal [93]. Top view and cross-sectional diagram of the smart lens sensor and optical image of the fabricated device. The smart lens consists of a 'sensing part' that displays color changes using photonic crystal (PC)-based flexible membrane and a 'contact part' that directly contacts with an eyeball and identifies its morphology change.

Researchers have also introduced emerging strain-sensitive materials, such as graphene nanowalls (GNWs) [94], to develop IOP sensors with high piezoresistive performance. By combining a Wheatstone-bridge strain-gauge circuit [95] with MEMS fabrication,

these designs produced highly sensitive smart contact lens sensors that maintained reliable readouts across different IOP fluctuation amplitudes and frequencies. Meanwhile, improving material fabrication methods can also enhance the sensitivity of IOP sensors. Zhu et al. [30] proposed a method for producing hydrogel-based smart contact lenses using a conformal stacking technique, addressing the challenges of hydrogel swelling and spherical integration of pyramidal microstructured dielectric elastomers. Researchers enhanced the sensitivity of a parallel-plate capacitive pressure sensor by placing a pyramidal microstructured dielectric elastomer between two electrodes on a spherical pHEMA hydrogel substrate.

In addition, colorimetric sensors have also been integrated into smart contact lens platforms for IOP detection [93,96,97]. On the basis of a biocompatible PHEMA hydrogel, Wang et al. [96] developed a structural color sensor that exhibited an excellent response to subtle changes in IOP and water content. Colorimetric smart contact lens sensors can work with smartphones, offering a simple route for ophthalmic health monitoring. Ye et al. [97] developed a dual-analyte smart contact lens sensor that simultaneously measures IOP and MMP-9. The device uses a three-dimensional periodic structure to generate structural color through selective light diffraction, thereby avoiding potentially harmful electronic components near the eye. Similarly, as shown in Figure 4e, researchers enhanced a photonic-crystal-based IOP sensor with a microhydraulic amplification mechanism [93]. The sensor reports IOP through visible color changes, requires neither an external power source nor wireless power-transfer components, and enables low-cost, non-invasive quantitative IOP measurement by analyzing RGB values captured with a smartphone camera. To compare the detection accuracy of various sensors, we have summarized the data in Table 1.

Table 1. Summary of smart contact lens IOP sensors.

Sensing Materials	Fabrication Methods	Detection Range	Detection Sensitivity	Ref.
Silica colloidal particles	Injection-molding method	7.5~30 mmHg	1.5 mm·Hg·nm^{-1}	[96]
Photonic crystal	Spin-casting method	3.2~5.12 mmHg	0.23 nm·mmHg^{-1}	[93]
Micropatterned PDMS and functionalized FET	Spin-casting method	0~40 mmHg	0.708 mm·mmHg^{-1}	[85]
Clearflex and NOA65	Lathe-cut method	10~40 mmHg	4.5 mm 1% strain^{-1}	[84]
Graphene	Spin-casting method	8~34 mmHg	150 μV mmHg^{-1}	[98]

3.2. Glucose

Currently, the most commonly used glucose testing method for diabetic patients is the finger-prick method. Long-term finger-prick sampling causes pain and inconvenience for patients [99]. Studies have revealed a significant correlation between tear glucose levels and blood glucose levels [100–104]. Although tear glucose levels cannot yet serve as a decisive indicator for distinguishing between diabetic and non-diabetic individuals [105], the non-invasive nature of tear glucose detection holds promise as a new approach for diabetes diagnosis.

Since its discovery, graphene has attracted considerable attention due to its unique structure and excellent electrical properties. Researchers have integrated graphene field-effect transistor (G-FET)-based glucose sensors into smart contact lens platforms. Although enzyme inactivation can compromise the specificity and stability of conventional G-FET sensors, and rigid substrates can reduce wearing comfort and user compliance, advances in materials and fabrication have enabled enzyme-free G-FET glucose sensors based on pyrene-1-boronic acid (PBA). This design uses PBA as a glucose-recognition layer and provides a more stable route for tear-glucose monitoring in wearable contact lenses [106]. This sensor exhibits a wide detection range of 1–5 μM, a high sensitivity of −0.6695 μA/decade, and a low detection limit of 0.1 μM, paving the way for the development and application of G-FET sensors in other body fluid analyses. Surface-enhanced Raman scattering (SERS) technology

has also contributed significantly to the advancement of smart contact lens glucose sensors. Lee et al. [107] constructed a multilayer structure consisting of a biocompatible silk fibroin layer, a 4-mercaptophenylboronic acid-coated silver nanowire layer that generates high-density hot spots for Raman signal enhancement, and a protective film. The SERS substrate showed a robust glucose response over 500 nM^{-1} mM, and tests with pre- and post-prandial human tears validated its glucose-sensing capability. These results highlight the potential of SERS for developing non-invasive smart contact lens sensors for tear-glucose monitoring. Furthermore, Luo et al. [108] provided a reliable and reproducible large-area SERS-active substrate fabrication technique, further confirming the potential of such SERS-based smart contact lens glucose sensors.

Hydrogel materials, typically derived from biological sources or synthesized as hydrophilic polymers, can form networks that absorb aqueous fluids. Their high hydrophilicity makes them highly suitable for ophthalmic applications [109]. Researchers commonly integrate hydrogels into contact lenses to monitor glucose levels in tear fluid. Kim et al. designed a smart contact lens based on hydrogel. The smart contact lens integrates gold-platinum bimetallic nano catalysts (HA-Au@Pt BiNCs) on a nanoporous hydrogel, allowing direct contact with the eye [110]. This biosensor achieves efficient glucose detection through a redox reaction catalyzed by glucose oxidase within the hydrogel, experimentally demonstrating a glucose sensitivity of 180.18 μA cm^2 mM^{-1}, a response time of 3.6 s, and a detection limit of 0.01 mg dL^{-1}, showcasing characteristics of high sensitivity, rapid response, and minimal hysteresis [111].

Electrochemical detection is one of the classical approaches for glucose sensing and can be classified into active and passive types based on the energy source [112–116]. Glucose oxidase (GOD) enables highly sensitive and selective glucose detection by catalyzing the oxidation of glucose to gluconic acid and hydrogen peroxide in the presence of water and oxygen [117]. Subsequently, the hydrogen peroxide undergoes an oxidation reaction at the anode of an electrochemical probe, generating a current proportional to the glucose concentration. This strategy allows a selective glucose fuel cell to harvest the generated current for power supply while simultaneously sensing glucose. As shown in Figure 5a, the device forms an accurate amperometric glucose sensor by coating a platinum working electrode with a chitosan–polyvinyl alcohol hydrogel containing co-immobilized glucose oxidase and bovine serum albumin, while using a silver/silver chloride layer as the reference electrode. Coupling this sensor with an electronically controlled drug-delivery module enables sensitive and stable tear-glucose monitoring and on-demand drug release [16]. As shown in Figure 5b, Park et al. designed an electrochemical glucose sensor and controlled drug release via wireless energy transfer, thereby enabling tear glucose monitoring and the treatment of diabetic retinopathy [13].

In addition to electrochemical detection based on GOD oxidation current, Li et al. [118] also proposed detecting glucose based on the colorimetric reaction of PB (Prussian blue) with the hydrogen peroxide produced by GOD-mediated glucose decomposition. To overcome the time-consuming calibration and signal instability of electrochemical sensors, researchers developed a photonic-microstructure-based smart contact lens sensor by microimprinting densely packed concave features into a phenylboronic-acid-functionalized hydrogel film [119]. The sensor quantifies glucose by measuring glucose-dependent changes in transmitted light intensity, and a smartphone photodiode enables portable readout.

Despite increasing attempts to use tears as a substitute for blood in diabetes diagnosis, controversy surrounding the correlation between tear glucose and blood glucose still limits the clinical use of tears. Recently, researchers developed a wireless, flexible smart contact lens sensor to clarify the relationship between blood glucose and tear glucose [12]. The study introduced the concept of a personalized lag time to account for the influence of reflex

tearing on tear-glucose dynamics and showed that the device could accurately predict blood glucose levels. As shown in Figure 5c, the platform integrates a Prussian blue and glucose-oxidase-modified electrochemical sensor, a resonant coil and a thinned NFC chip (NHS3152) onto a flexible contact lens substrate. This architecture enables battery-free operation through wireless power delivery and supports wireless data transmission with sufficient bandwidth. Continued advances in this field could make tear-glucose-based diabetes monitoring clinically feasible. Finally, we summarized the technical parameters of the glucose-detecting contact lenses in Table 2.

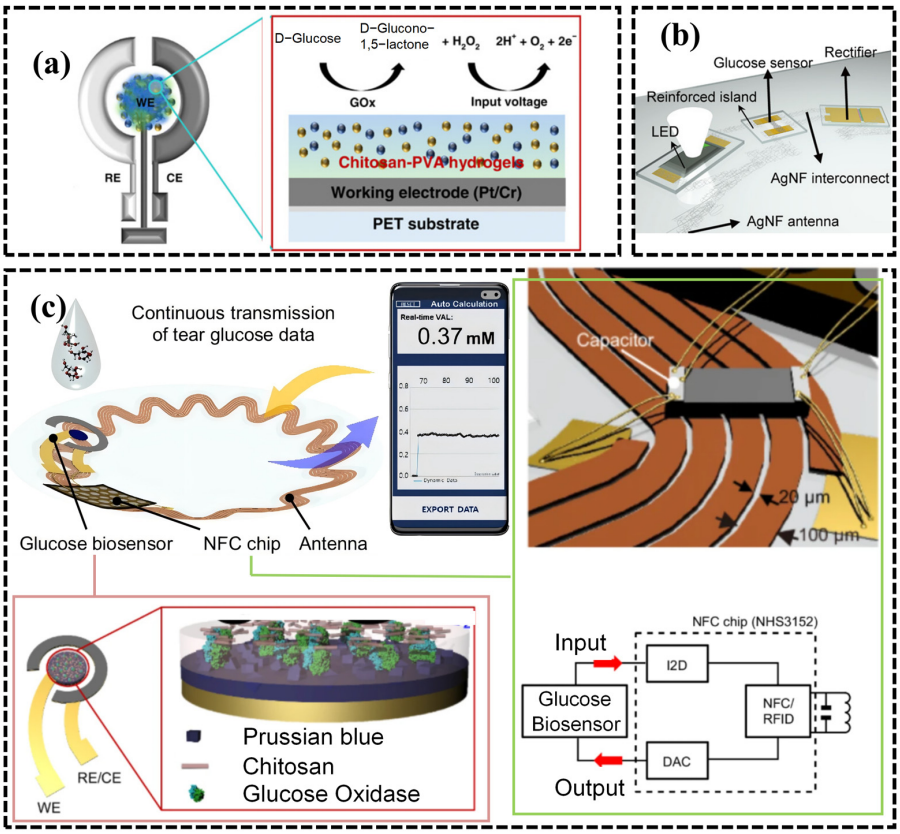


Figure 5. Application of intelligent contact lenses in tear glucose detection. (**a**) Schematic illustration of an ocular glucose sensor with three electrodes (WE, working electrode; RE, reference electrode; CE, counter electrode) and the mechanism of glucose measurement in tear fluid [16]. (**b**) Schematic image of the soft, smart contact lens. The rectifier, the LED, and the glucose sensor are located on the reinforced regions. The transparent, stretchable AgNF-based antenna and interconnects are located on an elastic region [13]. (**c**) Schematic of the SCL-based TG monitoring system, including smartphone-assisted wireless readout, a two-electrode electrochemical glucose biosensor, a magnified reaction layer on the working electrode, a serpentine antenna with an integrated capacitor, and the circuit design for wireless glucose monitoring [12].

Table 2. Summary of smart contact lens glucose sensors.

Sensing Materials	Fabrication Methods	Detection Range	Detection Sensitivity	Ref.
N-hydroxysuccinimide activated glucose probe	Injection-molding method	0.023~1.00 mmol·L^{-1}	9.3 μmol L^{-1}	[120]
Glucose oxidase	Lathe-cut method	0.10~0.60 mmol·L^{-1}	240 μA·cm^{-2}·mmol·L^{-1}	[116]
Graphene	Spin-casting method	0.10~0.90 mmol·L^{-1}	−22.72% mmol·L^{-1}	[13]
Photonic microstructure	-	0~5.00 mmol·L^{-1}	12 nm·mmol·L^{-1}	[121]
Hyaluronate modified gold@platinum bimetallic electrode	Injection-molding method	1.00~50.00 mg·dL^{-1}	110.92 μA·cm^{-2}·mmol·L^{-1}	[122]

3.3. Electrolytes and pH

The pH of tears in healthy individuals is approximately 7.4, whereas in patients with dry eye syndrome, tear pH can rise to 7.9, accompanied by elevated sodium ion concentrations [123]. Therefore, developing smart contact lens sensors capable of monitoring tear electrolyte concentrations and pH is crucial for providing timely and accurate guidance for patients with ocular diseases [124].

Researchers have integrated wearable colorimetric sensors into contact lenses to detect tear pH and various ions. For example, anthocyanin pigments change their chemical structure in response to hydrogen-ion concentration, making them attractive active materials for biocompatible pH sensors. As shown in Figure 6a, Riaz et al. [125] utilized naturally derived anthocyanins to develop a smart contact lens pH sensor whose color exhibited a systematic shift as a function of pH. In addition to such bioactive molecules applicable to pH detection, as shown in Figure 6b,c, Yetisen et al. [11] used phthalic acid as a pH probe to develop a fluorescent scleral lens sensor capable of quantitatively detecting pH and multiple ions (Na^+, K^+, Ca^{2+}, Mg^{2+}, and Zn^{2+}). Achieving continuous monitoring of tear composition within the physiological range has the potential to revolutionize the management of dry eye disease.

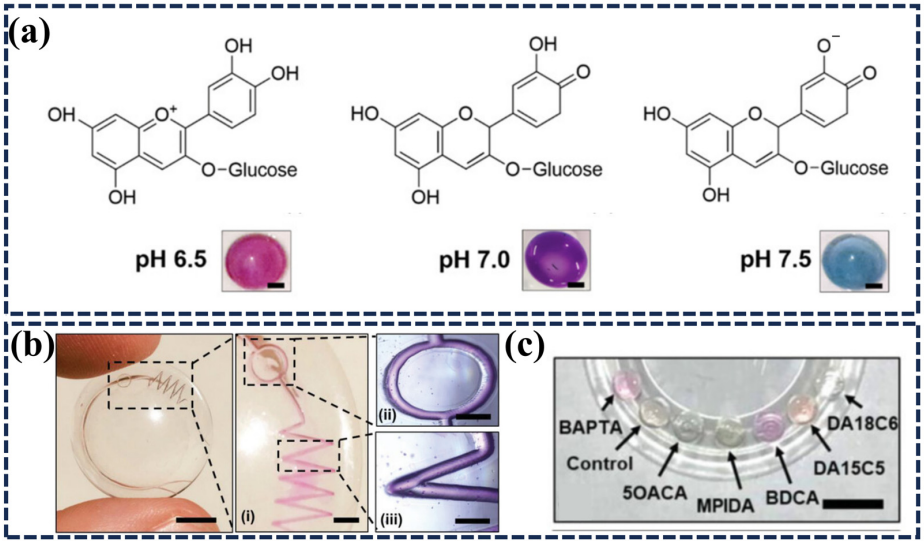


Figure 6. Application of smart contact lenses in tear pH and electrolyte detection. (**a**) Smart contact lens pH sensor based on natural anthocyanins [125]. Anthocyanin chemical formulas at physiological pH levels. Inset photographs show tinted contact lenses at different pH values. Scale bars: 5.0 mm. (**b**) Microchannel network and multiplexed sensing regions in the scleral lens for tear electrolyte analysis. The insets show: (**i**) the mixer and branching microchannels, (**ii**,**iii**) a magnified branching microchannel, and (**c**) a magnified mixer. The scleral lens contains fluorescent probes for pH, Na^+, K^+, Ca^{2+}, Mg^{2+}, and Zn^{2+} detection [11].

Researchers have also used microchannels fabricated by non-traditional manufacturing processes to measure tear osmolarity for dry-eye diagnosis. Moreddu's team [126] used a CO_2 laser to engrave microchannels consisting of a central ring and four branches onto commercial contact lenses, with biosensors embedded in the microcavities at the branch ends. A smartphone–MATLAB algorithm based on a nearest-neighbor model performed the colorimetric readout. In artificial tears, the sensor generated a response within 15 s and achieved a sensitivity of 12.23 nm pH^{-1} with a resolution of 0.25 pH units. As shown in Figure 6c, to expand in situ tear analysis, the same team [127] later integrated multiplexed paper-based microfluidics onto laser-engraved commercial contact lenses, realizing multiplexed detection of hydrogen ions, proteins, glucose, nitrite, and L-ascorbic acid. This

design prevents leakage and promotes capillary flow, yielding an improved pH sensitivity of 22 nm/pH and a resolution of 0.13 pH units.

The embedding of ion-responsive dyes as specific sensitive materials into contact lenses has been the subject of extensive research. Chen et al. [128] used high-resolution 3D printing and replica molding techniques to fabricate PHEMA hydrogel contact lenses containing microchannels, combining ion-sensitive dye-based colorimetric pH sensing with an electrochemical sodium ion sensor. This device could respond to pH over a range of 5–9 and sodium ion solutions at concentrations of 5–25 mM within approximately 5 min.

It is evident that current smart contact lens sensors for ion and pH detection remain limited to the fields of chromatography or spectroscopy. However, based on the previously discussed application of G-FET sensors in IOP and tear glucose monitoring, the use of G-FETs for pH and ion sensing is foreseeable [129].

3.4. Biomarkers

Cortisol is a steroid hormone secreted by the adrenal glands, triggered by psychological or physical stress [130]. Chronic stress leads to abnormal cortisol secretion, and the resulting cortisol accumulation increases the concentrations of lipids and amino acids, which in turn can lead to a surge of diseases such as Cushing's disease, cardiovascular complications, type 2 diabetes, and anxiety disorders. Researchers have therefore explored cortisol as a key biomarker for assessing individual stress levels and predicting outcomes after traumatic brain injury [131]. Beyond ocular biomarkers, cortisol sensing has also attracted increasing attention in wearable and non-invasive health monitoring. Researchers have rapidly developed cortisol sensors for blood, saliva, sweat, urine and other body fluids. Despite this progress, conventional sensing and analytical methods often show temperature-dependent performance and require bulky, complex equipment for sample extraction and analysis, which limits their use in personalized at-home health monitoring. Thus, it is essential to develop wearable devices capable of non-invasively and accurately monitoring cortisol concentrations. As shown in Figure 7a, Ku et al. [14] designed a flexible smart contact lens sensor based on a graphene field-effect transistor, integrating a transparent antenna and a wireless communication device, operable remotely via an external smartphone without obstructing the wearer's vision. In vivo experiments in live rabbits and a human pilot trial verified the biocompatibility of the device, providing a reliable solution for the non-invasive and continuous monitoring of cortisol.

The rising prevalence of chronic ocular surface inflammation (OSI) and the lack of reliable screening methods have stimulated improvements and developments in its diagnostic approaches [132]. Matrix metalloproteinase-9 (MMP-9) serves as a representative biomarker of ocular surface inflammation. Shin's team [133] proposed a novel smart contact lens sensor targeting MMP-9. The design crosslinks polyvinylacrylamide into a hydrogel matrix and conjugates MMP-9-cleavable fluorescent peptides to the network, enabling enzyme-responsive fluorescence readout. In the absence of the analyte, a quencher attached to the peptide suppressed the fluorescent signal; in the presence of MMP-9, it cleaved the hydrogel-conjugated peptide, resulting in detectable fluorescence. Although it possessed a detection range of 0–20 $\times$ 10^{-9} M and a detection limit of 4.02 $\times$ 10^{-9} M, it required surgical intervention. To avoid such invasiveness, Park et al. [49] developed a smart contact lens sensor that wirelessly integrates a diagnostic sensor with a therapeutic device. This system used an MMP-9 antibody-modified graphene field-effect transistor biosensor to measure MMP-9 levels in tear fluid. A continuous random network of ultra-long silver nanofibers (AgNF) electrospun on PDMS served as a stretchable transparent electrode, and a heating film was formed to provide high-temperature therapy. By integrating a wireless antenna, capacitors, resistors and an NFC chip, the device enables wireless power delivery,

data transmission and real-time automatic control of the heating film. In applications for multiplexed detection of MMP-9 and other pathological conditions, as shown in Figure 7b, Ye et al. [97] attempted to immobilize specific sequence fluorescent peptides onto AuNBs (gold nanobowls) as a SERS substrate. MMP-9 specifically recognized and cleaved the AuNBs at the Gly-Leu site, causing the release of the fluorescent peptide termini and a reduction in Raman intensity, achieving quantitative analysis of MMP-9 in tears with a detection limit as low as 1.29 ng/mL.

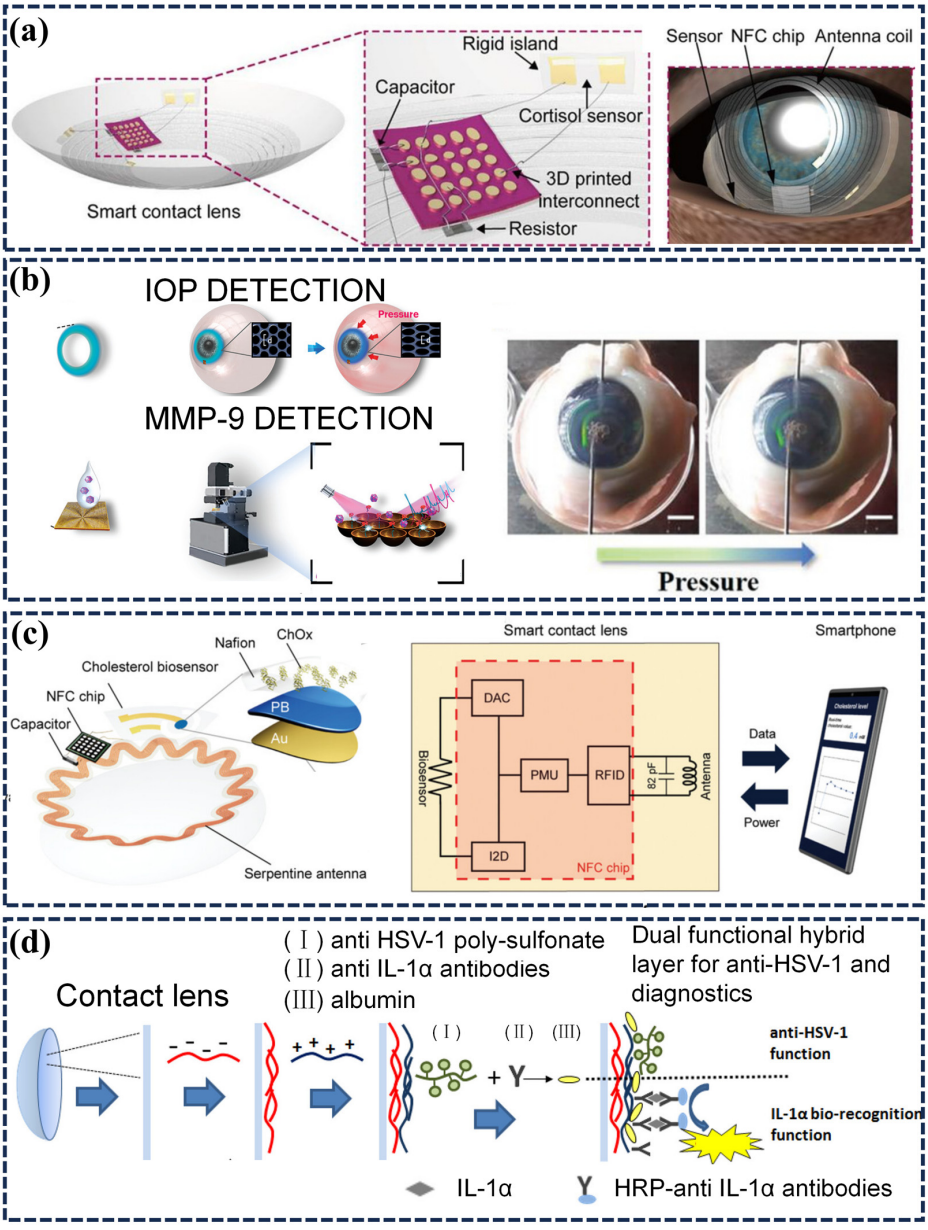


Figure 7. Application of smart contact lenses in tear biomarker detection. (**a**) Schematic of the packaged smart contact lens integrated with three-dimensional (3D) printed stretchable interconnects and a cortisol sensor located on the rigid island. A capacitor and a resistor were integrated for the resonance frequency and reference resistance, respectively [14]. (**b**) Dual-functional contact lens sensor integrating an antiopal structure for IOP monitoring and a peptide-functionalized AuNB SERS substrate for MMP-9 detection, with a representative photograph of structural-color-based real-time IOP monitoring on a porcine eye under increasing pressure. Scale bar, 5 mm [97]. (**c**) Smart contact lens incorporating a cholesterol biosensor with its enzymatic reaction scheme, together with a circuit diagram of the device [134]. (**d**) Schematic diagram illustrating the surface-engineering fabrication processes and construction of the theranostic lens [15].

According to data from the World Health Organization, cardiovascular diseases (CVDs) are the leading cause of premature death globally, accounting for 38% of all deaths in 2019. Hyperlipidemia is a strong risk factor for CVDs, typically caused by genetic or environmental factors, including elevated cholesterol concentrations resulting from unhealthy diets. Since hyperlipidemia presents no symptoms, and current standard methods for quantifying blood cholesterol, such as isotope dilution mass spectrometry and the modified Abell-Kendall method, require hospital or laboratory settings, while cholesterol levels fluctuate at any time due to lifestyle or daily dietary influences, there is a lack of corresponding point-of-care and mobile detection methods. As shown in Figure 7c, previous studies have demonstrated a correlation between free cholesterol in tears and blood cholesterol levels. A cholesterol-oxidase-based smart contact lens sensor integrated a serpentine stretchable antenna, capacitors and an NFC chip to enable wireless power delivery and smartphone-based data transmission. In vivo experiments using a rabbit model demonstrated the biocompatibility and reproducibility of the device, as well as the feasibility of this smart contact lens sensor for diagnosing hyperlipidemia through tear cholesterol measurement [128].

In herpes simplex keratitis (HSK), viral reactivation releases infectious viral particles and triggers ocular-surface inflammation, thereby driving disease recurrence. This process upregulates inflammatory cytokines such as interleukin-1α (IL-1α), which can serve as candidate biomarkers for diagnosing herpes simplex virus type 1 (HSV-1) infection. Mak et al. [10] developed a diagnostic-plus-therapeutic dual-function smart contact lens sensor constructed using a layer-by-layer surface engineering technique, as shown in Figure 7d. The device exhibited good surface wettability and optical transparency and was non-toxic to human corneal epithelial cells. The device also contained an antiviral coating, demonstrating effective anti-HSV-1 activity and a detection limit for IL-1α as low as 1.43 pg/mL. Its innovative concept of capturing and pre-concentrating biomarkers provided a new solution for the diagnosis of tear disease markers, overcoming the challenges of small tear sample volumes and low biomarker concentrations, and proving the practicability of smart contact lens theranostic devices as a new generation of wearable medical devices.

Beyond single sensing mechanisms, nanoengineered interfaces offer a new route for detecting ocular biomarkers by integrating multiple signal-transduction modes within one sensing platform. For example, a recent study used an on-chip nano-corrugated graphene interface to realize field-effect transistor, electrochemical and optical sensing on the same substrate [135]. The nanoscale corrugations enhanced charge transfer between biomolecules and graphene, reduced interfacial screening and generated optical responses that remained weak or absent in flat graphene. Although the platform did not target contact lens sensors, it establishes an important design principle for wearable ocular biosensors: rational interface engineering can improve detection sensitivity, expand signal readout modalities and enable simultaneous detection of multiple biochemical signals in miniaturized devices.

Therefore, we summarize the main strategies for detecting ocular biomarkers in Table 3, including optical, electrochemical, field-effect transistor-based, and colorimetric methods. Because each strategy offers distinct advantages and limitations, we present a tabulated comparison of key parameters to clarify their analytical performance, integration potential and translational constraints.

Table 3. Summary of technical specifications for smart contact lenses.

Approach	Sensing Material/Model	Target and Clinical Field	Detection Range	Sensitivity/LOD	Response Time or Reactivity Model	Wireless or Readout Mode	Ref.
Optical	**Stretchable PDMS nanopillar array/ strain-tunable diffraction grating**	**IOP monitoring for glaucoma**	**15–35 mmHg**	**Detection limit below 2 mmHg**	**Corneal/lens deformation changes grating pitch and diffraction color**	Smartphone color-recognition optical readout	[88]
Optical	N-hydroxysuccinimide activated glucose probe	Tear glucose monitoring for diabetes	0.1–1.0 mM	9.3 umol/L	Probe response to glucose concentration	Optical/smartphone-compatible readout described in glucose-sensing section	[120]
Optical	Photonic microstructure	Tear glucose monitoring for diabetes	0–50 mM	12 nm/mmol/L	Optical wave-length/color shift induced by glucose-responsive material	Smartphone-based optical readout	[121]
Colorimetric	CO_2-laser engraved microchannel contact lens	Tear pH/osmolarity-related dry-eye assessment	pH 6.0–8.0; glucose 0–20 mmol L^{-1}, protein 0.5–5.0 g L^{-1}	12.23 nm/pH; glucose: 1.4 nm $mmol^{-1}$ L,	Response within 15 s in artificial tears	Smartphone nearest-neighbor color analysis	[126]
Colorimetric/microfluidic	Paper-based microfluidics	Multiplexed tear analysis	Not reported in this review	22 nm/pH; 0.13 pH-unit resolution	Capillary-flow microfluidic colorimetric reaction	Smartphone/image-based color readout	[127]
Colorimetric/optical	Silica colloidal-particle structural color sensor	IOP	7.5–30 mmHg	1.5 mmHg/nm	Structural color changes under pressure/water-content variation	Smartphone-assisted visual/color readout	[96]
Colorimetric/optical	Photonic-crystal sensor	IOP monitoring for glaucoma	3.2–5.12 mmHg	0.23 nm/mmHg	Pressure-induced optical color/RGB shift	Power-free smartphone RGB analysis	[93]
FET-based	Graphene strain sensor	IOP monitoring	8–34 mmHg	150 uV/mmHg	Resistance/electrical response to corneal deformation	Electrical readout; wireless mode not specified in this review	[136]
FET-based	Graphene-based glucose sensor	Tear glucose	0.10–0.90 mmol/L	−22.72% $mmol/L^{-1}$	Glucose-induced electrical response	Wireless circuit/display integration reported for smart contact lens platform	[13]
Electrochemical	Glucose oxidase electrode	Tear glucose	0.10–0.60 mmol/L	240 uA cm^{-2} $mmol/L^{-1}$	Enzyme-catalyzed electrochemical reaction	Electrical readout; wireless mode not specified in this review	[116]
Electrochemical	Hyaluronate-modified Au@Pt bimetallic electrode	Tear glucose monitoring for diabetes	1.00–50.00 mg/dL	110.92 uA cm^{-2} $mmol/L^{-1}$	Electrocatalytic glucose response	Wireless smart contact lens platform	[122]

In summary, smart contact lens sensors, supported by new materials, flexible electronics, and tear biomarker discovery, have become an important direction in wearable medical devices. Their value should not be judged only by low detection limits or device miniaturization; it also depends on whether the measured tear signal can be linked reproducibly to ocular disease status, systemic physiology, or treatment response.

The diagnostic potential of tear biomarkers should therefore be framed cautiously. Tear composition changes with blinking, reflex tearing, evaporation, ocular surface inflammation, sampling method, lens wear, and circadian or metabolic state. Biomarkers such as glucose, cortisol, cholesterol, and inflammatory cytokines may correlate with blood levels or disease severity in selected settings, but these relationships are not universal surrogates. Future studies should report paired tear–blood or tear–clinical datasets, sampling conditions, lag time, and inter-individual variability before proposing stand-alone diagnostic thresholds.

4. Challenges and Outlook

Despite the impressive progress made in material innovation and application expansion, smart contact lenses still face multiple challenges on the path from laboratory prototypes to clinical translation and commercialization. These barriers are not limited to sensor performance, but also involve power delivery, wireless communication, long-term ocular safety, device stability, manufacturing reproducibility and clinical validation. The following sections discuss three key aspects: power supply and data transmission, biocompatibility and interface safety, and tear-sample characteristics and accurate detection.

4.1. Power Supply and Data Transmission

Power delivery remains one of the most restrictive factors for smart contact lenses because the device must operate on a thin, soft, transparent and curved ocular interface. Conventional wired power supplies are incompatible with natural eye movement and daily wear, and may cause discomfort, corneal abrasion or infection risk. Wireless power delivery, including radio-frequency, magnetic-resonance, photovoltaic and inductive coupling strategies, provides a more suitable route, but each approach has specific limitations. For example, miniaturized antenna coils or NFC modules are constrained by the limited lens area and curvature, which can reduce coupling efficiency and make power transfer sensitive to eye movement, blinking, eyelid shielding and coil misalignment. Excessive power density or impedance mismatch may also induce Joule heating, leading to local temperature increases and potential corneal irritation.

Data transmission is another major challenge. Optical and colorimetric sensors often require external cameras, stable illumination and image-processing algorithms, making the readout sensitive to ambient light, viewing angle, eyelid coverage and motion artifacts. Electrochemical sensors require stable low-noise circuits, reliable wireless communication and correction for signal drift during long-term wear. In addition, packet loss, electromagnetic interference and unstable coupling distance may reduce data continuity during real-time monitoring. Therefore, future systems should integrate low-power circuit design, stable wireless links, temperature control, motion-tolerant readout algorithms and user-friendly interfaces. For translational use, these systems must also be compatible with smartphones or portable readers, operate safely under daily activities, and meet electrical, thermal and wireless-safety requirements.

4.2. Biocompatibility and Interface Safety

Biocompatibility is a central challenge because smart contact lenses must remain in direct contact with the cornea and tear film. Conventional contact-lens parameters, including

oxygen permeability, water content, wettability, modulus, curvature and thickness, become more difficult to optimize after sensors, electrodes, antennas, chips or encapsulation layers are embedded. Reduced oxygen transmissibility may cause corneal hypoxia, whereas insufficient wettability and tear exchange can induce dry-eye symptoms and discomfort. Mechanical mismatch between rigid electronic components and the soft lens matrix may generate local stress concentration, especially during blinking and eye rotation, increasing the risk of friction damage or corneal irritation.

The ocular environment also imposes chemical and biological challenges. Tear electrolytes may corrode electrodes, conductive traces and interconnects, while proteins, lipids and mucins can adsorb onto sensor surfaces and cause biofouling, signal attenuation or baseline drift. Encapsulation layers must therefore prevent leakage, corrosion and delamination while maintaining flexibility, transparency, oxygen permeability and sensing access to tear biomarkers. Stretchable electrodes, serpentine interconnects and kirigami-inspired layouts can reduce mechanical mismatch, but their long-term reliability under repeated blinking, rubbing, cleaning, storage and sterilization remains insufficiently validated. From a translational perspective, future devices need standardized assessments of cytotoxicity, irritation, sensitization, oxygen permeability, extractables and leachables, as well as repeated-wear studies under realistic ocular conditions.

4.3. Tear Sample Characteristics and Accurate Detection

Accurate detection in tear fluid is challenging because the available sample volume is extremely small and biomarker concentrations are often lower than those in blood. The total tear volume is only approximately 7 μL per eye, and the volume that can be collected or accessed by a contact lens sensor is even smaller. Such limited sample availability places high demands on sensor sensitivity, anti-interference capability and signal-to-noise ratio. For biomarkers such as glucose, cortisol, inflammatory cytokines and proteins, the concentration in tears can be affected by dilution, tear turnover, evaporation and reflex tearing, making direct quantitative interpretation difficult.

Tear composition is also highly dynamic. Environmental stimuli, dry-eye conditions, irritation, blinking frequency, circadian rhythm, inflammation, medication and contact-lens wear itself can all alter tear secretion and biomarker levels. In addition, several systemic biomarkers exhibit a time delay or weak correlation between blood and tear concentrations, which complicates their use for disease diagnosis or treatment guidance. For example, tear glucose is generally much lower than blood glucose and may not change synchronously with blood glucose. Therefore, smart contact lens sensors should not rely only on single-point calibration or short-term proof-of-concept tests. Future studies should include long-term calibration stability, intra- and inter-individual variability, interference from tear components, comparison with clinical gold-standard assays, and validation in relevant patient populations.

For clinical translation, detection accuracy must be evaluated not only by analytical metrics such as sensitivity, limit of detection, selectivity and response time, but also by clinically relevant metrics, including reproducibility across users, false-positive and false-negative rates, diagnostic thresholds, data interpretation algorithms and compatibility with routine clinical workflows. Combining multimodal sensing, reference channels, on-lens calibration, anti-fouling interfaces and machine-learning-assisted signal correction may improve reliability. However, large-scale clinical studies are still required to determine whether tear-based and ocular signals measured by smart contact lenses can provide robust diagnostic or monitoring value in real-world settings.

4.4. Outlook

As a cutting-edge technology integrating biomedicine, microelectronics, and materials science, smart contact lenses, despite the many issues and challenges mentioned above, hold tremendous potential as a key enabling technology for medical monitoring and personalized health management. Focusing on the following key future development directions may give rise to highly transformative application prospects.

First, it is necessary to optimize NFC or RF energy transmission technology to improve energy transfer efficiency, while reducing local Joule heating through a distributed coil layout. Developing biofuel cells using electrolytes or glucose in tear fluid, or driving the device with the kinetic energy of blinking, is also a possible means to achieve self-powering. Second, developing flexible substrates with high oxygen permeability, wettability, and elastic deformability that support long-term embedding of electronic components, while utilizing stretchable electronics to reduce friction from electronic components and circuits, and developing reliable thin-film encapsulation schemes to isolate electrolytes from contact with electronic components, are necessary paths to improve the biocompatibility of smart contact lenses.

To meet the demands of accurate detection, it is necessary to introduce novel nanomaterials, enzyme amplification techniques, or field enhancement effects to improve sensor sensitivity, or to establish adaptive models from the perspective of analyte pre-concentration to achieve reliable detection of low-concentration samples. Employing multi-parameter and dynamic calibration algorithms can address the problems of analyte concentration variation over time and fluctuations due to environmental changes. Using cloud-based big data analytics to build personalized calibration models can reduce the impact of individual differences and provide accurate diagnostic results and health management recommendations.

Beyond sensing performance, developers must address practical and regulatory barriers before smart contact lenses can enter clinical use. They should evaluate long-term wear under conditions that mimic daily use, including blinking, tear exchange, corneal oxygen supply, lens dehydration, protein deposition, eye rubbing and repeated insertion or removal. Manufacturers must also design sterilization, packaging and storage procedures that preserve enzymes, dyes, nanomaterials, electrodes and wireless components, while pre-market testing should verify batch-to-batch reproducibility, signal stability and shelf-life reliability. Robust calibration will be essential because tear volume, evaporation, ambient light, temperature, ocular curvature, blinking frequency and individual tear composition can all shift sensor baselines. Future systems should therefore integrate reference channels, drift-correction algorithms and user-specific calibration models to support reliable quantitative interpretation. Wireless and smartphone-connected lenses will also require data security by design, including encrypted transmission, privacy-preserving storage, informed consent and controlled access to health records. Regulatory approval will depend on standardized evidence of biocompatibility, optical safety, electrical safety, sterilization tolerance, analytical accuracy and clinical validity. Scalable translation will further require sensing modules that fit existing contact lens manufacturing workflows, including molding, curing, hydration, sterilization and packaging, without compromising transparency, oxygen permeability, mechanical comfort or production yield. These logistical requirements will determine whether smart contact lenses remain laboratory prototypes or become clinically deployable ocular health-monitoring platforms.

Following the trend of wearable medical device development, achieving integrated diagnosis and treatment is the ultimate goal of smart contact lenses. Although some related combined diagnostic and therapeutic wearable medical device application studies currently exist, they are mostly a superposition of diagnostic and therapeutic functions, coexisting in parallel. Future integrated diagnostic and therapeutic smart contact lenses must realize the

organic unification of treatment strategies that are feedback-controlled by diagnostic results, achieving a shift from home monitoring to home medical care. In addition, developing holographic projection display technology to support augmented reality functions such as navigation and information prompts can enable smart contact lenses to transcend the medical field and transform people's lives in broader domains.

Author Contributions: Conceptualization, L.G. and J.D.; writing—original draft preparation, L.G. and J.D.; writing—review and editing, L.G. and Y.W.; supervision, Y.W. All authors have read and agreed to the published version of the manuscript.

Funding: This research was funded by Beijing Municipal Science & Technology Commission, Administrative Commission of Zhongguancun Science Park (No. Z251100006025016), National Natural Science Foundation of China (No. 62471017), Beijing Natural Science Foundation (No. L246068), Shandong Provincial Natural Science Foundation (No. ZR2024QF030), the Fundamental Research Funds for the Central Universities.

Institutional Review Board Statement: Not applicable.

Informed Consent Statement: Not applicable.

Data Availability Statement: Data will be made available on request.

Conflicts of Interest: The authors declare no conflicts of interest.

Abbreviation

3D	three-dimensional
AgNF	silver nanofiber
AuNB	gold nanobowl
BWMF-CLS	bilateral-wall microfluidic contact lens sensor
CB	carboxybetaine
CE	counter electrode
CMOS	complementary metal-oxide-semiconductor
CNT	carbon nanotube
CVD	cardiovascular disease
EGDMA	ethylene glycol dimethacrylate
FBG	fiber Bragg grating
FET	field-effect transistor
G-FET	graphene field-effect transistor
GMA	glycidyl methacrylate
GNWs	graphene nanowalls
GOD	glucose oxidase
HA	hyaluronate
HEMA	2-hydroxyethyl methacrylate
HSK	herpes simplex keratitis
HSV-1	herpes simplex virus type 1
IL-1α	interleukin-1 alpha
IOP	intraocular pressure
LCR	inductor-capacitor-resistor
LOD	limit of detection
MA	methacrylic acid
MATLAB	Matrix Laboratory
MEMS	microelectromechanical systems
MMP-9	matrix metalloproteinase-9
MPC	2-methacryloyloxyethyl phosphorylcholine
NFC	near-field communication

NHS	N-hydroxysuccinimide
NOA65	Norland Optical Adhesive 65
NVP	N-vinylpyrrolidone
OSI	ocular surface inflammation
PBA	Prussian blue analog
PB	Prussian blue
PCBDA	poly(carboxybetaine-co-dopamine methacrylamide)
PC	photonic crystal
PDMS	polydimethylsiloxane
PEGMA	poly(ethylene glycol) methyl ether acrylate
pH	potential of hydrogen
PHEMA/pHEMA	poly(2-hydroxyethyl methacrylate)
PMMA	poly(methyl methacrylate)
PMAA	poly(methacrylic acid)
PVA	poly(vinyl alcohol)
PVCL	poly(N-vinylcaprolactam)
PVDF	poly(vinylidene fluoride)
RE	reference electrode
RF	radio frequency
RGB	red-green-blue
ROI	region of interest
SERS	surface-enhanced Raman scattering
Si-NR	silicon nanoribbon
UV	ultraviolet
WE	working electrode
WHO	World Health Organization
WMCL	wireless measuring contact lens

References

1. Sunwoo, S.-H.; Ha, K.-H.; Lee, S.; Lu, N.; Kim, D.-H. Wearable and implantable soft bioelectronics: Device designs and material strategies. *Annu. Rev. Chem. Biomol. Eng.* **2021**, *12*, 359–391. [CrossRef]
2. Shirzaei Sani, E.; Xu, C.; Wang, C.; Song, Y.; Min, J.; Tu, J.; Solomon, S.A.; Li, J.; Banks, J.L.; Armstrong, D.G.; et al. A stretchable wireless wearable bioelectronic system for multiplexed monitoring and combination treatment of infected chronic wounds. *Sci. Adv.* **2023**, *9*, eadf7388. [CrossRef] [PubMed]
3. Wang, M.; Yang, Y.; Min, J.; Song, Y.; Tu, J.; Mukasa, D.; Ye, C.; Xu, C.; Heflin, N.; McCune, J.S.; et al. A wearable electrochemical biosensor for the monitoring of metabolites and nutrients. *Nat. Biomed. Eng.* **2022**, *6*, 1225–1235. [CrossRef] [PubMed]
4. Lin, Y.; Bariya, M.; Javey, A.J.A.F.M. Wearable biosensors for body computing. *Adv. Funct. Mater.* **2021**, *31*, 2008087. [CrossRef]
5. De la Paz, E.; Maganti, N.H.; Trifonov, A.; Jeerapan, I.; Mahato, K.; Yin, L.; Sonsa-ard, T.; Ma, N.; Jung, W.; Burns, R.; et al. A self-powered ingestible wireless biosensing system for real-time in situ monitoring of gastrointestinal tract metabolites. *Nat. Commun.* **2022**, *13*, 7405. [CrossRef] [PubMed]
6. Lin, Y.; Xiang, S.; Zou, W.; Chen, X.; Gao, F.; Liu, Y.; Sun, Y.; Chen, P.; Zhang, Q.; Han, X.; et al. Magneto-elastic for wireless intraocular pressure monitoring. *Chem. Eng. J.* **2024**, *498*, 155357. [CrossRef]
7. Wang, J.; Liu, X.J.; Diao, K.; Wang, S. Liquid-alloy-based dual sensing elements contact lens sensor for continuous intraocular pressure monitoring. *Measurement* **2025**, *240*, 115392. [CrossRef]
8. Kaya, O.; Aydin, M.A.; Teymoori, M.; Erden, O.K.; Sadeghzadeh, S.; Dedeoglu, U.O.; Demir, S.; Muhikanci, O.; Sahin, A.; Torun, H.; et al. A first-in-human pilot study of a novel electrically-passive metamaterial-inspired resonator-based ocular sensor embedded contact lens monitoring intraocular pressure fluctuations. *Contact Lens Anterior Eye* **2024**, *47*, 102102. [CrossRef] [PubMed]
9. Chen, W.; Chen, S.; Zhao, X.; Yang, L.; Zhao, Y.; Wei, R.; Wu, J. Kirigami Design Smart Contact Lens for Highly Sensitive Eyelid Pressure Measurement. *ACS Sens.* **2024**, *10*, 814–824. [CrossRef] [PubMed]
10. Shao, Y.; Hu, B.; Liu, X.; Ni, Z.; Shu, Y.; Zhang, X.; Shen, J.; Liang, L.; Zhou, L.; Liu, J.; et al. Multi-functional, conformal systems with ultrathin crystalline-silicon-based bioelectronics for characterization of intraocular pressure and ocular surface temperature. *Biosens. Bioelectron.* **2025**, *267*, 116786. [CrossRef] [PubMed]

11. Yetisen, A.K.; Jiang, N.; Gonzalez, C.M.C.; Erenoglu, Z.I.; Dong, J.; Dong, X.; Stößer, S.; Brischwein, M.; Butt, H.; Cordeiro, M.F.; et al. Scleral Lens Sensor for Ocular Electrolyte Analysis. *Adv. Mater.* **2020**, *32*, 1906762. [CrossRef]
12. Park, W.; Seo, H.; Kim, J.; Hong, Y.-M.; Song, H.; Joo, B.J.; Kim, S.; Kim, E.; Yae, C.-G.; Kim, J.; et al. In-depth correlation analysis between tear glucose and blood glucose using a wireless smart contact lens. *Nat. Commun.* **2024**, *15*, 2828. [CrossRef] [PubMed]
13. Park, J.; Kim, J.; Kim, S.; Cheong, W.H.; Jang, J.; Park, Y.-G.; Na, K.; Kim, Y.; Heo, J.H.; Lee, C.Y.; et al. Soft, smart contact lenses with integrations of wireless circuits, glucose sensors, and displays. *Sci. Adv.* **2018**, *4*, eaap9841. [CrossRef] [PubMed]
14. Ku, M.; Kim, J.; Won, J.; Kang, W.; Park, Y.; Park, J.; Lee, J.; Cheon, J.; Lee, H.H.; Park, J. Smart, soft contact lens for wireless immunosensing of cortisol. *Sci. Adv.* **2020**, *6*, eabb2891. [CrossRef] [PubMed]
15. Mak, W.C.; Cheung, K.Y.; Orban, J.; Lee, C.-J.; Turner, A.P.F.; Griffith, M. Surface-Engineered Contact Lens as an Advanced Theranostic Platform for Modulation and Detection of Viral Infection. *ACS Appl. Mater. Interfaces* **2015**, *7*, 25487–25494. [CrossRef] [PubMed]
16. Keum, D.H.; Kim, S.; Koo, J.; Lee, G.; Jeon, C.; Mok, J.W.; Mun, B.H.; Lee, K.J.; Kamrani, E.; Joo, C.-K.; et al. Wireless smart contact lens for diabetic diagnosis and therapy. *Sci. Adv.* **2020**, *6*, eaba3252. [CrossRef] [PubMed]
17. Alam, F.; Elsherif, M.; AiQattan, B.; Salih, A.; Lee, S.M.; Yetisen, A.K.; Park, S.; Butt, H. 3D Printed Contact Lenses. *ACS Biomater. Sci. Eng.* **2021**, *7*, 794–803. [CrossRef] [PubMed]
18. Farandos, N.M.; Yetisen, A.K.; Monteiro, M.J.; Lowe, C.R.; Yun, S.H. Contact Lens Sensors in Ocular Diagnostics. *Adv. Healthc. Mater.* **2015**, *4*, 792–810. [CrossRef]
19. McMahon, T.T.; Zadnik, K. Twenty-five years of contact lenses—The impact on the cornea and ophthalmic practice. *Cornea* **2000**, *19*, 730–740. [CrossRef] [PubMed]
20. Musgrave, C.S.A.; Fang, F. Contact Lens Materials: A Materials Science Perspective. *Materials* **2019**, *12*, 261. [CrossRef] [PubMed]
21. Ma, X.; Ahadian, S.; Liu, S.; Zhang, J.; Liu, S.; Cao, T.; Lin, W.; Wu, D.; de Barros, N.R.; Zare, M.R.; et al. Smart Contact Lenses for Biosensing Applications. *Adv. Intell. Syst.* **2021**, *3*, 2000263. [CrossRef]
22. Alipour, F.; Khaheshi, S.; Soleimanzadeh, M.; Heidarzadeh, S.; Heydarzadeh, S. Contact Lens-related Complications: A Review. *J. Ophthalmic Vis. Res.* **2017**, *12*, 193–204. [CrossRef] [PubMed]
23. Desai, A.R.; Maulvi, F.A.; Desai, D.M.; Shukla, M.R.; Ranch, K.M.; Vyas, B.A.; Shah, S.A.; Sandeman, S.; Shah, D.O. Multiple drug delivery from the drug-implants-laden silicone contact lens: Addressing the issue of burst drug release. *Mater. Sci. Eng. C* **2020**, *112*, 110885. [CrossRef] [PubMed]
24. Tran, N.P.D.; Yang, M.C.; Tran-Nguyen, P.L. Evaluation of silicone hydrogel contact lenses based on poly (dimethylsiloxane) dialkanol and hydrophilic polymers. *Colloids Surf. B-Biointerfaces* **2021**, *206*, 111957. [CrossRef] [PubMed]
25. Melendez Ortiz, H.I.; Alvarez Lorenzo, C.; Concheiro, A.; Bucio, E. Grafting of N-vinyl caprolactam and methacrylic acid onto silicone rubber films for drug-eluting products. *J. Appl. Polym. Sci.* **2015**, *132*, 41855. [CrossRef]
26. Wang, J.J.; Liu, F. Photoinduced graft polymerization of 2-methacryloyloxyethyl phosphorylcholine on silicone hydrogels for reducing protein adsorption. *J. Mater. Sci.-Mater. Med.* **2011**, *22*, 2651–2657. [CrossRef] [PubMed]
27. Wang, J.J.; Liu, F. Imparting antifouling properties of silicone hydrogels by grafting poly(ethylene glycol) methyl ether acrylate initiated by UV light. *J. Appl. Polym. Sci.* **2012**, *125*, 548–554. [CrossRef]
28. Valint, P.L.; Ammon, D.M.; McGee, J.A.; Grobe, G.L.; Ozark, R.M. Surface Treatment for Silicone Hydrogel Contact Lenses Comprising Hydrophilic Polymer Chains Attached to an Intermediate Carbon Coating. U.S. Patent 06902812, 7 June 2005.
29. Valint, P.L., Jr.; Grobe, G.L., III; Ammon, D.M., Jr.; McGee, J.A. Plasma Surface Treatment of Silicone Hydrogel Contact Lenses with a Flexible Carbon Coating. U.S. Patent 6213604, 10 April 2001.
30. Zhu, H.; Yang, H.; Zhan, L.; Chen, Y.; Wang, J.; Xu, F. Hydrogel-Based Smart Contact Lens for Highly Sensitive Wireless Intraocular Pressure Monitoring. *ACS Sens.* **2022**, *7*, 3014–3022. [CrossRef] [PubMed]
31. Shaker, L.M.M.; Al-Azzawi, W.K.; Al-Amiery, A.; Takriff, M.S.S.; Isahak, W.N.R.W. Highly transparent antibacterial hydrogel-polymeric contact lenses doped with silver nanoparticles. *J. Vinyl Addit. Technol.* **2023**, *29*, 1023–1035. [CrossRef]
32. Tong, W.Y.; Tan, W.N.; Azizi, M.A.K.; Leong, C.R.; El Azab, I.H.; Lim, J.W.; Mahmoud, M.H.H.; Dailin, D.J.; Ibrahim, M.M.; Chuah, L.F. Nanoparticle-laden contact lens for controlled release of vancomycin with enhanced antibiotic efficacy. *Chemosphere* **2023**, *338*, 139492. [CrossRef] [PubMed]
33. Zha, X.; Zhang, S.; Pu, J.; Zhao, X.; Ke, K.; Bao, R.; Bai, L.; Liu, Z.; Yang, M.; Yang, W. Nanofibrillar Poly(vinyl alcohol) Ionic Organohydrogels for Smart Contact Lens and Human-Interactive Sensing. *ACS Appl. Mater. Interfaces* **2020**, *12*, 23514–23522. [CrossRef] [PubMed]
34. Wang, Z.; Wang, X.; Zhou, Y.; Zhang, X.; Bian, Y.; Lin, Q.; Wang, Y.; Sheng, R. Dual-functional hCe-pHEMA contact lenses for ocular antibiotic release, antioxidant protection, and in vivo corneal bacterial infection treatment. *J. Control. Release* **2025**, *383*, 113813. [CrossRef] [PubMed]
35. Vasquez Quintero, A.; Arai, R.; Yamazaki, Y.; Sato, T.; De Smet, H. Near-Field Communication Powered Hydrogel-Based Smart Contact Lens. *Adv. Mater. Technol.* **2020**, *5*, 2000702. [CrossRef]

36. Maldonado Codina, C.; Efron, N. Dynamic wettability of pHEMA-based hydrogel contact lenses. *Ophthalmic Physiol. Opt.* **2006**, *26*, 408–418. [CrossRef] [PubMed]
37. Seo, E.; Kumar, S.; Lee, J.; Jang, J.; Park, J.H.; Chang, M.C.; Kwon, I.; Lee, J.S.; Huh, Y.I. Modified Hydrogels Based on Poly(2-hydroxyethyl methacrylate) (pHEMA) with Higher Surface Wettability and Mechanical Properties. *Macromol. Res.* **2017**, *25*, 704–711. [CrossRef]
38. Ketelson, H.A.; Meadows, D.L.; Stone, R.P. Dynamic wettability properties of a soft contact lens hydrogel. *Colloids Surf. B Biointerfaces* **2005**, *40*, 1–9. [CrossRef] [PubMed]
39. Li, R.C.; Guan, X.P.; Lin, X.L.; Guan, P.Y.; Zhang, X.; Rao, Z.Q.; Du, L.; Zhao, J.F.; Rong, J.H.; Zhao, J.H. Poly(2-hydroxyethyl methacrylate)/β-cyclodextrin-hyaluronan contact lens with tear protein adsorption resistance and sustained drug delivery for ophthalmic diseases. *Acta Biomater.* **2020**, *110*, 105–118. [CrossRef] [PubMed]
40. Tranoudis, I.; Efron, N. Parameter stability of soft contact lenses made from different materials. *Contact Lens Anterior Eye J. Br. Contact Lens Assoc.* **2004**, *27*, 115–131. [CrossRef] [PubMed]
41. Li, Z.G.; Cheng, H.W.; Ke, L.J.; Liu, M.T.; Wang, C.G.; Loh, X.J.; Li, Z.B.; Wu, Y.L. Recent Advances in New Copolymer Hydrogel-Formed Contact Lenses for Ophthalmic Drug Delivery. *Chemnanomat* **2021**, *7*, 564–579. [CrossRef]
42. Hyon, S.H.; Cha, W.I.; Ikada, Y.; Kita, M.; Ogura, Y.; Honda, Y. POLY(VINYL ALCOHOL) HYDROGELS AS SOFT CONTACT-LENS MATERIAL. *J. Biomater. Sci.-Polym. Ed.* **1994**, *5*, 397–406. [CrossRef] [PubMed]
43. Baker, M.I.; Walsh, S.P.; Schwartz, Z.; Boyan, B.D. A review of polyvinyl alcohol and its uses in cartilage and orthopedic applications. *J. Biomed. Mater. Res. Part B Appl. Biomater.* **2012**, *100B*, 1451–1457. [CrossRef] [PubMed]
44. Sahabudeen, H.; Machatschek, R.; Lendlein, A. Multifunctionality as design principle for contact lens materials. *Multifunct. Mater.* **2021**, *4*, 042001. [CrossRef]
45. Mutlu, Z.; Es-haghi, S.S.; Cakmak, M. Recent Trends in Advanced Contact Lenses. *Adv. Healthc. Mater.* **2019**, *8*, 1801390. [CrossRef] [PubMed]
46. Alam, F.; Elsherif, M.; AlQattan, B.; Ali, M.; Ahmed, I.M.G.; Salih, A.; Antonysamy, D.S.; Yetisen, A.K.; Park, S.; Butt, H. Prospects for Additive Manufacturing in Contact Lens Devices. *Adv. Eng. Mater.* **2021**, *23*, 2000941. [CrossRef]
47. Manabe, K.; Matsuda, M.; Nakamura, C.; Takahashi, K.; Kyung, K.-H.; Shiratori, S. Antifibrinogen, Antireflective, Antifogging Surfaces with Biocompatible Nano-Ordered Hierarchical Texture Fabricated by Layer-by-Layer Self-Assembly. *Chem. Mater.* **2017**, *29*, 4745–4753. [CrossRef]
48. Liu, G.Y.; Li, K.J.; Wang, H.B.; Ma, L.; Yu, L.; Nie, Y. Stable Fabrication of Zwitterionic Coating Based on Copper-Phenolic Networks on Contact Lens with Improved Surface Wettability and Broad-Spectrum Antimicrobial Activity. *ACS Appl. Mater. Interfaces* **2020**, *12*, 16125–16136. [CrossRef] [PubMed]
49. Jang, J.; Kim, J.; Shin, H.; Park, Y.-G.; Joo, B.J.; Seo, H.; Won, J.-e.; Kim, D.W.; Lee, C.Y.; Kim, H.K.; et al. Smart contact lens and transparent heat patch for remote monitoring and therapy of chronic ocular surface inflammation using mobiles. *Sci. Adv.* **2021**, *7*, eabf7194. [CrossRef] [PubMed]
50. Goto, E.; Tagami, T.; Ogawa, K.; Ozeki, T. Fabrication of 3D-Printed Contact Lens Composed of Polyethylene Glycol Diacrylate for Controlled Release of Azithromycin. *Biol. Pharm. Bull.* **2023**, *46*, 1461–1467. [CrossRef] [PubMed]
51. Li, B.J.; Guo, M.Q.; Wang, X.J.; Qiao, L.Y.; Song, H.; Li, Z.Q. Design and 3D Printing of Soft Orthokeratology Lenses. *ACS Appl. Mater. Interfaces* **2025**, *17*, 31368–31379. [CrossRef] [PubMed]
52. Zidan, G.; Greene, C.A.; Etxabide, A.; Rupenthal, I.D.; Seyfoddin, A. Gelatine-based drug-eluting bandage contact lenses: Effect of PEGDA concentration and manufacturing technique. *Int. J. Pharm.* **2021**, *599*, 120452. [CrossRef] [PubMed]
53. Childs, A.; Li, H.; Lewittes, D.M.; Dong, B.; Liu, W.; Shu, X.; Sun, C.; Zhang, H.F. Fabricating customized hydrogel contact lens. *Sci. Rep.* **2016**, *6*, 34905. [CrossRef] [PubMed]
54. Maldonado Codina, C.; Efron, N. Impact of manufacturing technology and material composition on the mechanical properties of hydrogel contact lenses. *Ophthalmic Physiol. Opt.* **2004**, *24*, 551–561. [CrossRef] [PubMed]
55. Maulvi, F.A.; Singhania, S.S.; Desai, A.R.; Shukla, M.R.; Tannk, A.S.; Ranch, K.M.; Vyas, B.A.; Shah, D.O. Contact lenses with dual drug delivery for the treatment of bacterial conjunctivitis. *Int. J. Pharm.* **2018**, *548*, 139–150. [CrossRef] [PubMed]
56. Li, D.; Wei, Q.; Wu, C.; Zhang, X.; Xue, Q.; Zheng, T.; Cao, M. Superhydrophilicity and strong salt-affinity: Zwitterionic polymer grafted surfaces with significant potentials particularly in biological systems. *Adv. Colloid Interface Sci.* **2020**, *278*, 102141. [CrossRef] [PubMed]
57. Zhu, Y.; Li, S.; Li, J.; Falcone, N.; Cui, Q.; Shah, S.; Hartel, M.C.; Yu, N.; Young, P.; Barros, N.R.; et al. Lab-on-a-Contact Lens: Recent Advances and Future Opportunities in Diagnostics and Therapeutics. *Adv. Mater.* **2022**, *34*, 2108389. [CrossRef] [PubMed]
58. Leonardi, M.; Leuenberger, P.; Bertrand, D.; Bertsch, A.; Renaud, P. First steps toward noninvasive intraocular pressure monitoring with a sensing contact lens. *Investig. Ophthalmol. Vis. Sci.* **2004**, *45*, 3113–3117. [CrossRef] [PubMed]
59. Chu, M.X.; Miyajima, K.; Takahashi, D.; Arakawa, T.; Sano, K.; Sawada, S.-i.; Kudo, H.; Iwasaki, Y.; Akiyoshi, K.; Mochizuki, M.; et al. Soft contact lens biosensor for in situ monitoring of tear glucose as non-invasive blood sugar assessment. *Talanta* **2011**, *83*, 960–965. [CrossRef] [PubMed]

60. Fan, Y.; Tu, H.; Zhao, H.; Wei, F.; Yang, Y.; Ren, T. A wearable contact lens sensor for noninvasive in-situ monitoring of intraocular pressure. *Nanotechnology* **2021**, *32*, 095106. [CrossRef] [PubMed]
61. Dou, Z.; Tang, J.; Liu, Z.; Sun, Q.; Wang, Y.; Li, Y.; Yuan, M.; Wu, H.; Wang, Y.; Pei, W.; et al. Wearable Contact Lens Sensor for Non-Invasive Continuous Monitoring of Intraocular Pressure. *Micromachines* **2021**, *12*, 108. [CrossRef] [PubMed]
62. Yun, J.; Zeng, Y.P.; Kim, M.; Gao, C.T.; Kim, Y.; Lu, L.; Kim, T.T.H.; Zhao, W.T.; Bae, T.H.; Lee, S.W. Tear-Based Aqueous Batteries for Smart Contact Lenses Enabled by Prussian Blue Analogue Nanocomposites. *Nano Lett.* **2021**, *21*, 1659–1665. [CrossRef] [PubMed]
63. Zhu, H.; Yang, H.; Xu, S.; Ma, Y.; Zhu, S.; Mao, Z.; Chen, W.; Hu, Z.; Pan, R.; Xu, Y.; et al. Frequency-encoded eye tracking smart contact lens for human-machine interaction. *Nat. Commun.* **2024**, *15*, 3588. [CrossRef] [PubMed]
64. Tsai, C.W.; Hsu, S.H.; Huang, Y.C.; Yeh, G.T.; Huang, Y.H.; Hsu, C.Y.; Wu, C.Y.; Yang, J.J.; Zhang, X.W.; Chiou, J.C. A Semi-Passive Smart Contact Lens with on-Lens Power Storage Element. *IEEJ Trans. Electr. Electron. Eng.* **2024**, *19*, 852–858. [CrossRef]
65. Seo, D.; Neely, R.M.; Shen, K.; Singhal, U.; Alon, E.; Rabaey, J.M.; Carmena, J.M.; Maharbiz, M.M. Wireless Recording in the Peripheral Nervous System with Ultrasonic Neural Dust. *Neuron* **2016**, *91*, 529–539. [CrossRef] [PubMed]
66. Khan, S.R.; Pavuluri, S.K.; Cummins, G.; Desmulliez, M.P.Y. Wireless Power Transfer Techniques for Implantable Medical Devices: A Review. *Sensors* **2020**, *20*, 3487. [CrossRef] [PubMed]
67. Charthad, J.; Chang, T.C.; Liu, Z.K.; Sawaby, A.; Weber, M.J.; Baker, S.; Gore, F.; Felt, S.A.; Arbabian, A. A mm-Sized Wireless Implantable Device for Electrical Stimulation of Peripheral Nerves. *IEEE Trans. Biomed. Circuits Syst.* **2018**, *12*, 257–270. [CrossRef] [PubMed]
68. Ma, C.B.; Shang, X.D.; Sun, M.M.; Bo, X.J.; Bai, J.; Du, Y.; Zhou, M. Emerging Multifunctional Wearable Sensors: Integrating Multimodal Sweat Analysis and Advanced Material Technologies for Next-Generation Health Monitoring. *ACS Sens.* **2025**, *10*, 2388–2408. [CrossRef] [PubMed]
69. Brasier, N.; Frobert, O.; De Ieso, F.; Meyer, D.; Kowatsch, T.; Ghaffari, R. The potential of wearable sweat sensors in heart failure management. *Nat. Electron.* **2024**, *7*, 182–184. [CrossRef]
70. Chen, Y.; Wan, X.H.; Li, G.L.; Ye, J.Q.; Gao, J.; Wen, D. Metal Hydrogel-Based Integrated Wearable Biofuel Cell for Self-Powered Epidermal Sweat Biomarker Monitoring. *Adv. Funct. Mater.* **2024**, *34*, 2404329. [CrossRef]
71. Shi, Y.Q.; Hu, Y.B.; Zhang, Y.H.; Tjandra, A.D.; Park, S.; Chandrawati, R.; Tasoglu, S.; Jiang, N.; Yetisen, A.K. Microfluidic contact lens for continuous monitoring of ocular oxidative stress. *Biosens. Bioelectron.* **2025**, *280*, 117427. [CrossRef] [PubMed]
72. Yin, S.N.; Chen, X.F.; Li, R.Z.; Sun, L.L.; Yao, C.Y.; Li, Z. Wearable, Biocompatible, and Dual-Emission Ocular Multisensor Patch for Continuous Profiling of Fluoroquinolone Antibiotics in Tears. *ACS Nano* **2024**, *18*, 18522–18533. [CrossRef] [PubMed]
73. Chen, T.J.; Pang, J.; Liu, X.C.; Chen, N.; Wu, C.C.; Duan, Y.; You, X.F.; Dou, Q.; Yuan, C.; Wang, Y.X.; et al. Anti-biofilm super-hydrophilic gel sensor for saliva glucose monitoring. *Nano Today* **2024**, *55*, 102141. [CrossRef]
74. Liu, R.; Nie, Q.L.; Wang, Y.H.Z.; Wu, Y.; Tu, Y.T.; Xie, C.L.; Xiao, X.F.; You, R.Y.; Lu, Y.D. Diaper-based wearable SERS sensing system with a silver nano dual-structure composite hydrogel for the detection of biomarkers and pH in urine. *Chem. Eng. J.* **2024**, *498*, 155207. [CrossRef]
75. Song, S.J.; Zhou, W.H.; Wei, X.Y.; Zhao, H.J.; Hu, D.; Liu, J.Q.; Zhang, X.; Yu, S.; Yang, F.C. A Janus Fabric with Hexagonal Microcavity Channels for Efficient Urine Transport and Accurate Physiological Monitoring. *ACS Sens.* **2025**, *10*, 2113–2124. [CrossRef] [PubMed]
76. Wang, K.; Liu, W.J.; Wu, J.Z.; Li, H.; Peng, H.; Zhang, J.H.; Ding, K.; Wang, X.X.; Hou, C.Y.; Zhang, H.; et al. Smart Wearable Sensor Fuels Noninvasive Body Fluid Analysis. *ACS Appl. Mater. Interfaces* **2025**, *17*, 13279–13301. [CrossRef] [PubMed]
77. Brasier, N.; Wang, J.; Gao, W.; Sempionatto, J.R.; Dincer, C.; Ates, H.C.; Guder, F.; Olenik, S.; Schauwecker, I.; Schaffarczyk, D.; et al. Applied body-fluid analysis by wearable devices. *Nature* **2024**, *636*, 57–68. [CrossRef] [PubMed]
78. Yadav, K.S.; Rajpurohit, R.; Sharma, S. Glaucoma: Current treatment and impact of advanced drug delivery systems. *Life Sci.* **2019**, *221*, 362–376. [CrossRef] [PubMed]
79. Tektas, O.Y.; Lütjen-Drecoll, E. Structural changes of the trabecular meshwork in different kinds of glaucoma. *Exp. Eye Res.* **2009**, *88*, 769–775. [CrossRef] [PubMed]
80. Pardianto, G. Recent awareness and consideration of intraocular pressure fluctuation during eye surgery. *J. Cataract. Refract. Surg.* **2015**, *41*, 695. [CrossRef] [PubMed]
81. Detry Morel, M. Update in tonometry. Phosphene and rebound tonometries, self-tonometry and technologies for the future. *Bull. Soc. Belg. D'ophtalmologie* **2007**, 87–95.
82. An, H.; Wang, X.; Liao, Z.; Zhang, L.; Zhao, H.; Yang, Y.; Song, J.; Ma, Y. LC contact lens sensor for ultrasensitive intraocular pressure monitoring. *npj Flex. Electron.* **2024**, *8*, 53. [CrossRef]
83. Song, C.; Ben Shlomo, G.; Que, L. A Multifunctional Smart Soft Contact Lens Device Enabled by Nanopore Thin Film for Glaucoma Diagnostics and In Situ Drug Delivery. *J. Microelectromechanical Syst.* **2019**, *28*, 810–816. [CrossRef]
84. Agaoglu, S.; Diep, P.; Martini, M.; Samudhyatha, K.T.; Baday, M.; Araci, I.E. Ultra-sensitive microfluidic wearable strain sensor for intraocular pressure monitoring. *Lab A Chip* **2018**, *18*, 3471–3483. [CrossRef] [PubMed]

85. An, H.; Chen, L.; Liu, X.; Zhao, B.; Zhang, H.; Wu, Z. Microfluidic contact lenses for unpowered, continuous and non-invasive intraocular pressure monitoring. *Sens. Actuators A-Phys.* **2019**, *295*, 177–187. [CrossRef]
86. Yuan, M.; Liu, Z.D.; Wu, X.T.; Gou, H.Y.; Zhang, Y.G.; Ning, X.; Li, W.J.; Yao, Z.H.; Wang, Y.J.; Pei, W.H.; et al. High-sensitive microfluidic contact lens sensor for intraocular pressure visualized monitoring. *Sens. Actuators A-Phys.* **2023**, *354*, 114250. [CrossRef]
87. Li, Y.; Li, L.; Ye, Z.; Zhang, H.; Sun, X.; Li, C.; Gui, L. A Novel Implantable Piezoresistive Microsensor for Intraocular Pressure Measurement. *ACS Sens.* **2024**, *9*, 3958–3966. [CrossRef] [PubMed]
88. Moreddu, R.; Mahmoodi, N.; Kassanos, P.; Vigolo, D.; Mendes, P.M.; Yetisen, A.K. Stretchable Nanostructures as Optomechanical Strain Sensors for Ophthalmic Applications. *ACS Appl. Polym. Mater.* **2021**, *3*, 5416–5424. [CrossRef]
89. Kouhani, M.H.M.; Wu, J.J.; Tavakoli, A.; Weber, A.J.; Li, W. Wireless, passive strain sensor in a doughnut-shaped contact lens for continuous non-invasive self-monitoring of intraocular pressure. *Lab A Chip* **2020**, *20*, 332–342. [CrossRef] [PubMed]
90. Kumuda, S.; Uma, G.; Umapathy, M.; Anand, V.R.; Ramanan, S.R.; Asokan, S.; Rajanna, K. Non-invasive FBG-based contact lens for continuous intraocular pressure monitoring. *Opt. Fiber Technol.* **2024**, *84*, 103777. [CrossRef]
91. Kim, J.; Park, J.; Park, Y.-G.; Cha, E.; Ku, M.; An, H.S.; Lee, K.-P.; Huh, M.-I.; Kim, J.; Kim, T.-S.; et al. A soft and transparent contact lens for the wireless quantitative monitoring of intraocular pressure. *Nat. Biomed. Eng.* **2021**, *5*, 772–782. [CrossRef] [PubMed]
92. Li, X.; Chen, W.; Li, H.; Shen, B.; He, J.; Gao, H.; Bin, F.; Li, H.; Xiao, D. Temperature Self-Compensating Intelligent Wireless Measuring Contact Lens for Quantitative Intraocular Pressure Monitoring. *Acs Appl. Mater. Interfaces* **2024**, *16*, 22522–22531. [CrossRef] [PubMed]
93. Maeng, B.; Chang, H.K.; Park, J. Photonic crystal-based smart contact lens for continuous intraocular pressure monitoring. *Lab A Chip* **2020**, *20*, 1740–1750. [CrossRef] [PubMed]
94. Liu, Z.; Wang, G.; Pei, W.; Wei, C.; Wu, X.; Dou, Z.; Li, Y.; Wang, Y.; Chen, H. Application of graphene nanowalls in an intraocular pressure sensor. *J. Mater. Chem. B* **2020**, *8*, 8794–8802. [CrossRef] [PubMed]
95. Liu, Z.; Wang, G.; Ye, C.; Sun, H.; Pei, W.; Wei, C.; Dai, W.; Dou, Z.; Sun, Q.; Lin, C.-T.; et al. An Ultrasensitive Contact Lens Sensor Based On Self-Assembly Graphene For Continuous Intraocular Pressure Monitoring. *Adv. Funct. Mater.* **2021**, *31*, 2010991. [CrossRef]
96. Wang, Y.; Zhao, Q.; Du, X. Structurally coloured contact lens sensor for point-of-care ophthalmic health monitoring. *J. Mater. Chem. B* **2020**, *8*, 3519–3526. [CrossRef] [PubMed]
97. Ye, Y.; Ge, Y.; Zhang, Q.; Yuan, M.; Cai, Y.; Li, K.; Li, Y.; Xie, R.; Xu, C.; Jiang, D.; et al. Smart Contact Lens with Dual-Sensing Platform for Monitoring Intraocular Pressure and Matrix Metalloproteinase-9. *Adv. Sci.* **2022**, *9*, 2104738. [CrossRef] [PubMed]
98. Xu, J.; Cui, T.; Hirtz, T.; Qiao, Y.; Li, X.; Zhong, F.; Han, X.; Yang, Y.; Zhang, S.; Ren, T.-L. Highly Transparent and Sensitive Graphene Sensors for Continuous and Non-invasive Intraocular Pressure Monitoring. *ACS Appl. Mater. Interfaces* **2020**, *12*, 18375–18384. [CrossRef] [PubMed]
99. Oliver, N.S.; Toumazou, C.; Cass, A.E.G.; Johnston, D.G. Glucose sensors: A review of current and emerging technology. *Diabet. Med.* **2009**, *26*, 197–210. [CrossRef] [PubMed]
100. Lane, J.D.; Krumholz, D.M.; Sack, R.A.; Morris, C. Tear glucose dynamics in diabetes mellitus. *Curr. Eye Res.* **2006**, *31*, 895–901. [CrossRef] [PubMed]
101. Aihara, M.; Kubota, N.; Minami, T.; Shirakawa, R.; Sakurai, Y.; Hayashi, T.; Iwamoto, M.; Takamoto, I.; Kubota, T.; Suzuki, R.; et al. Association between tear and blood glucose concentrations: Random intercept model adjusted with confounders in tear samples negative for occult blood. *J. Diabetes Investig.* **2021**, *12*, 266–276. [CrossRef] [PubMed]
102. La Belle, J.T.; Adams, A.; Lin, C.-E.; Engelschall, E.; Pratta, B.; Cook, C.B. Self-monitoring of tear glucose: The development of a tear based glucose sensor as an alternative to self-monitoring of blood glucose. *Chem. Commun.* **2016**, *52*, 9197–9204. [CrossRef] [PubMed]
103. Guo, S.; Wu, K.; Li, C.; Wang, H.; Sun, Z.; Xi, D.; Zhang, S.; Ding, W.; Zaghloul, M.E.; Wang, C.; et al. Integrated contact lens sensor system based on multifunctional ultrathin MoS_2 transistors. *Matter* **2021**, *4*, 969–985. [CrossRef] [PubMed]
104. Kim, S.; Jeon, H.J.; Park, S.; Lee, D.Y.; Chung, E. Tear Glucose Measurement by Reflectance Spectrum of a Nanoparticle Embedded Contact Lens. *Sci. Rep.* **2020**, *10*, 8254. [CrossRef] [PubMed]
105. Barrettino, D. Look into my eyes. *IEEE Spectr.* **2017**, *54*, 38–43. [CrossRef]
106. Zhi, Y.; Jian, J.; Qiao, Y.; Tian, Y.; Yang, Y.; Ren, T.-L. An ultrathin flexible affinity-based graphene field-effect transistor for glucose monitoring. In Proceedings of the 21st International Conference on Electronic Packaging Technology (ICEPT), Guangzhou, China, 12–15 August 2020; pp. 1–6.
107. Lee, W.C.; Koh, E.H.; Kim, D.H.; Park, S.G.; Jung, H.S. Plasmonic contact lens materials for glucose sensing in human tears. *Sens. Actuator B-Chem.* **2021**, *344*, 130297. [CrossRef]
108. Luo, S.; Mancini, A.; Lian, E.; Xu, W.; Berte, R.; Li, Y. Large Area Patterning of Highly Reproducible and Sensitive SERS Sensors Based on 10-nm Annular Gap Arrays. *Nanomaterials* **2022**, *12*, 3842. [CrossRef] [PubMed]

109. Fea, A.M.; Novarese, C.; Caselgrandi, P.; Boscia, G. Glaucoma Treatment and Hydrogel: Current Insights and State of the Art. *Gels* **2022**, *8*, 510. [CrossRef] [PubMed]
110. Kim, S.-K.; Lee, G.-H.; Jeon, C.; Han, H.H.; Kim, S.-J.; Mok, J.W.; Choun-Ki, J.; Shin, S.; Sim, J.-Y.; Myung, D.; et al. Bimetallic Nanocatalysts Immobilized in Nanoporous Hydrogels for Long-Term Robust Continuous Glucose Monitoring of Smart Contact Lens. *Adv. Mater.* **2022**, *34*, 10536. [CrossRef] [PubMed]
111. Hong, S.; Yu, T.; Wang, Z.; Lee, C.H. Biomaterials for reliable wearable health monitoring: Applications in skin and eye integration. *Biomaterials* **2025**, *314*, 122862. [CrossRef] [PubMed]
112. Zhou, Y.; Li, L.; Tong, J.L.; Chen, X.L.; Deng, W.; Chen, Z.Y.; Xiao, X.Y.; Yin, Y.; Zhou, Q.S.; Gao, Y.L.; et al. Advanced nanomaterials for electrochemical sensors: Application in wearable tear glucose sensing technology. *J. Mater. Chem. B* **2024**, *12*, 6774–6804. [CrossRef] [PubMed]
113. Jarnda, K.V.; Wang, D.; Qurrat-Ul-Ain, R.; Anaman, R.; Johnson, V.E.; Roberts, G.P.; Johnson, P.S.; Jallawide, B.W., Jr.; Kai, T.; Ding, P. Recent advances in electrochemical non-enzymatic glucose sensor for the detection of glucose in tears and saliva: A Review. *Sens. Actuators A-Phys.* **2023**, *363*, 114778. [CrossRef]
114. Peng, B.; Lu, J.; Balijepalli, A.S.; Major, T.C.; Cohan, B.E.; Meyerhoff, M.E. Evaluation of enzyme-based tear glucose electrochemical sensors over a wide range of blood glucose concentrations. *Biosens. Bioelectron.* **2013**, *49*, 204–209. [CrossRef] [PubMed]
115. Liao, Y.T.; Yao, H.; Lingley, A.; Parviz, B.; Otis, B.P. A 3-μW CMOS Glucose Sensor for Wireless Contact-Lens Tear Glucose Monitoring. *IEEE J. Solid-State Circuits* **2012**, *47*, 335–344. [CrossRef]
116. Yao, H.; Shum, A.J.; Cowan, M.; Lähdesmäki, I.; Parviz, B.A. A contact lens with embedded sensor for monitoring tear glucose level. *Biosens. Bioelectron.* **2011**, *26*, 3290–3296. [CrossRef] [PubMed]
117. Gonzales, W.V.; Mobashsher, A.T.; Abbosh, A. The Progress of Glucose MonitoringA Review of Invasive to Minimally and Non-Invasive Techniques, Devices and Sensors. *Sensors* **2019**, *19*, 800. [CrossRef] [PubMed]
118. Li, Z.; Yun, J.; Li, X.; Kim, M.; Li, J.; Lee, D.; Wu, A.; Lee, S.W. Power-Free Contact Lens for Glucose Sensing. *Adv. Funct. Mater.* **2023**, *33*, 2304647. [CrossRef]
119. Elsherif, M.; Hassan, M.U.; Yetisen, A.K.; Butt, H. Glucose Sensing with Phenylboronic Acid Functionalized Hydrogel-Based Optical Diffusers. *Acs Nano* **2018**, *12*, 2283–2291. [CrossRef] [PubMed]
120. Deng, M.; Song, G.; Zhong, K.; Wang, Z.; Xia, X.; Tian, Y. Wearable fluorescent contact lenses for monitoring glucose via a smartphone. *Sens. Actuator B-Chem.* **2022**, *352*, 131067. [CrossRef]
121. Elsherif, M.; Hassan, M.U.; Yetisen, A.K.; Butt, H. Wearable Contact Lens Biosensors for Continuous Glucose Monitoring Using Smartphones. *ACS Nano* **2018**, *12*, 5452–5462. [CrossRef] [PubMed]
122. Han, H.H.; Kim, S.-K.; Kim, S.-J.; Choi, I.; Mok, J.W.; Joo, C.-K.; Shin, S.; Hahn, S.K. Long-term stable wireless smart contact lens for robust digital diabetes diagnosis. *Biomaterials* **2023**, *302*, 122315. [CrossRef] [PubMed]
123. Yetisen, A.K.; Jiang, N.; Tamayol, A.; Ruiz-Esparza, G.U.; Zhang, Y.S.; Medina-Pando, S.; Gupta, A.; Wolffsohn, J.S.; Butt, H.; Khademhosseini, A.; et al. Paper-based microfluidic system for tear electrolyte analysis. *Lab A Chip* **2017**, *17*, 1137–1148. [CrossRef] [PubMed]
124. Badugu, R.; Jeng, B.H.; Reece, E.A.; Lakowicz, J.R. Contact lens to measure individual ion concentrations in tears and applications to dry eye disease. *Anal. Biochem.* **2018**, *542*, 84–94. [CrossRef] [PubMed]
125. Riaz, R.S.; Elsherif, M.; Moreddu, R.; Rashid, I.; Hassan, M.U.; Yetisen, A.K.; Butt, H. Anthocyanin-Functionalized Contact Lens Sensors for Ocular pH Monitoring. *ACS Omega* **2019**, *4*, 21792–21798. [CrossRef] [PubMed]
126. Moreddu, R.; Wolffsohn, J.S.; Vigolo, D.; Yetisen, A.K. Laser-inscribed contact lens sensors for the detection of analytes in the tear fluid. *Sens. Actuator B-Chem.* **2020**, *317*, 128183. [CrossRef]
127. Moreddu, R.; Elsherif, M.; Adams, H.; Moschou, D.; Cordeiro, M.F.; Wolffsohn, J.S.; Vigolo, D.; Butt, H.; Cooper, J.M.; Yetisen, A.K. Integration of paper microfluidic sensors into contact lenses for tear fluid analysis. *Lab A Chip* **2020**, *20*, 3970–3979. [CrossRef] [PubMed]
128. Chen, Y.; Zhang, S.; Cui, Q.; Ni, J.; Wang, X.; Cheng, X.; Alem, H.; Tebon, P.; Xu, C.; Guo, C.; et al. Microengineered poly(HEMA) hydrogels for wearable contact lens biosensing. *Lab A Chip* **2020**, *20*, 4205–4214. [CrossRef] [PubMed]
129. Holicky, M.; Fenech-Salerno, B.; Cass, A.E.G.; Torrisi, F. Fabrication of graphene field effect transistors on complex non-planar surfaces. *Appl. Phys. Lett.* **2024**, *125*, 113301. [CrossRef]
130. Holsboer, F.; Ising, M. Stress Hormone Regulation: Biological Role and Translation into Therapy. *Annu. Rev. Psychol.* **2010**, *61*, 81–109. [CrossRef] [PubMed]
131. Alkozi, H.A.; Alhudhayf, H.A.; Alawad, N.M.A. Association Between Dry Eye Disease with Anxiety and Depression Among Medical Sciences Students in Qassim Region: Cortisol Levels in Tears as a Stress Biomarker. *J. Multidiscip. Healthc.* **2024**, *17*, 4549–4557. [CrossRef] [PubMed]
132. Lanza, N.L.; Valenzuela, F.; Perez, V.L.; Galor, A. The Matrix Metalloproteinase 9 Point-of-Care Test in Dry Eye. *Ocul. Surf.* **2016**, *14*, 189–195. [CrossRef] [PubMed]

133. Shin, M.K.; Ji, Y.W.; Moon, C.-E.; Lee, H.; Kang, B.; Jinn, W.S.; Ki, J.; Mun, B.; Kim, M.-H.; Lee, H.K.; et al. Matrix metalloproteinase 9-activatable peptide-conjugated hydrogel-based fluorogenic intraocular-lens sensor. *Biosens. Bioelectron.* **2020**, *162*, 112254. [CrossRef] [PubMed]
134. Song, H.; Shin, H.; Seo, H.; Park, W.; Joo, B.J.; Kim, J.; Kim, J.; Kim, H.K.; Kim, J.; Park, J.-U. Wireless Non-Invasive Monitoring of Cholesterol Using a Smart Contact Lens. *Adv. Sci.* **2022**, *9*, 2203597. [CrossRef] [PubMed]
135. Nik Zulkarnine, N.H.; Faramarzi, V.; Huang, S.; Chandrasekar, N.; Perala, R.S.; Park, J.S.; Koprowski, K.; Chen, S.; Zhang, Y.; Darsi, S.; et al. Multi-modal biosensing enabled by on-chip nano-corrugated graphene. *Device* **2025**, *3*, 100572. [CrossRef]
136. Wang, R.; Xu, W.; Chen, D.; Zhou, R.; Wang, Q.; Gao, W.; Kono, J.; Xie, L.; Ying, Y. Ultrahigh-Sensitivity Molecular Sensing with Carbon Nanotube Terahertz Metamaterials. *ACS Appl. Mater. Interfaces* **2020**, *12*, 40629–40634. [CrossRef] [PubMed]

Disclaimer/Publisher's Note: The statements, opinions and data contained in all publications are solely those of the individual author(s) and contributor(s) and not of MDPI and/or the editor(s). MDPI and/or the editor(s) disclaim responsibility for any injury to people or property resulting from any ideas, methods, instructions or products referred to in the content.